Spring 5-1-2009

SYNTHESIS OF DIRUTHENIUM COMPLEXES AS CONNECTABLE MOLECULAR COMPONENTS

George Ling

SYNTHESIS OF DIRUTHENIUM COMPLEXES AS CONNECTABLE MOLECULAR COMPONENTS

A Capstone Project Submitted in Partial Fulfillment of the Requirements of the Renée Crown University Honors Program at Syracuse University

George Ling

Candidate for B.S. Degree in Chemistry with Honors

May 2009

Honors Capstone Project in Chemistry

APPROVED

Thesis Project Advisor: _____
Dr. Michael B. Sponsler

Honors Reader: _____
Dr. Mathew Maye

Honors Director:_____
Samuel Gorovitz

Date:_____

Abstract:

There have been great advances in electronics and technology within the last few years. The field of nanotechnology can further improve electronics in terms of efficiency, size and costs. There exist nanowires and nanotransistors that could accomplish this, however there exists no good method of connecting the two components together. Using the bottom-up approach and chemical synthesis, the goal is to synthesize molecular jumper cables and connectable molecular components (CMCs).

The template of the CMC will have two ruthenium (Ru) metal centers connected by a conjugated, organic bridge. Coordinated to the ruthenium metal centers will be different ligands that affect the properties of the complex. Many methods of synthesis exist to allow design of the given template. The reactions and methods studied were olefin metathesis for metal incorporation (OMMI) using Grubbs catalysts, metal hydride reactions, and organic reactions such as radical and substitution reactions. The ligands studied were aurophilic and pincer ligands. These ligands contain outward-directed lone pairs that will aid in single molecule conductivity studies. The ligands were methylthio-1,4-diphenyl-1H-1,2,4-triazolylidene, bipyridine, pyrazine, 2,6-bis(chloromethyl)pyrazine, 2,6-bis(diphenylphosphinomethyl)pyrazine, and 2,6-bis((diphenylphosphino)methyl)pyridine.

Complexes were characterized by proton nuclear magnetic resonance spectroscopy (^{1}H NMR), ultraviolet-visible spectroscopy (UV-Vis), infrared spectroscopy (IR), cyclic voltammetry (CV), atomic force microscopy (AFM), and ab-initio calculations using Gaussian 03W were also conducted. If successful, the last study to be conducted is single molecule conductivity studies in collaboration with a research group from Arizona State University. ^{1}H NMR was used to monitor reaction progress and along with IR spectroscopy, we were able to identify the complexes synthesized. UV-Vis spectroscopy provided information on the electronic structure of the complexes while CV provided information on redox stability and redox potentials. AFM provided information on topography and Gaussian allowed us to compare effects of different ligands, such as stability, upon coordination to the complexes.

The complexes synthesized using Grubbs catalysts and OMMI were unsuccessfully isolated. The greatest obstacle was stability, with many of the complexes decomposing over time. The complexes of the metal hydride insertion reactions were plagued with solubility and purification problems. However, a diruthenium complex was discovered to show potential as a CMC. In addition to the above obstacles, another problem was synthesis of the desired ligands that restricted the range and progress of the project. However, the project has yet to exhaust all the options and there are many other approaches and methods that will be investigated.

Table of Contents:

Section	Pages
1. Acknowledgements	i
2. Chapter 1: State of Nanotechnology	1-2
3. Chapter 2: General Template for Design	2-3
4. Chapter 3: Grubbs Catalyst and OMMI	
3.1- Background and Application in Project	3-5
3.2- Experimental Methods	5-8
3.3- Results and Discussion	9-11
5. Chapter 4: Hydride Insertion Reactions and Ab-Initio Studies	
4.1- Background	11-12
4.2- Experimental Section	12-19
4.3- Results and Discussion	19-30
6. Chapter 5: Incorporation of Pincer Ligands	
5.1- Background	30-31
5.2- Experimental Section	31-36
5.3- Results and Discussion	36-44
7. Discussion and Conclusion	45-46
8. Sources Cited and Consulted	47-48
9. Appendices	48-52
10. Written Summary of Capstone Project	53-57

Acknowledgements:

I would like to thank Dr. Sponsler for allowing me the opportunity to join his research group and partake in his research. It was with your guidance and expertise that I was able to accomplish as much as I have in my research. Others in the group I would like to thank are En Ma, Dr. Min-Chul Chung, Sarah Bolton, and Danielle Schuehler for their instruction and advice in the laboratory. Much thanks to Dr. Maye for allocating a part of his busy schedule to read my thesis and provide feedback. In addition, thank you to Dr. Freedman and Dr. Nafie for permitting me to use their laboratory and providing their expertise on Gaussian 03W. Last but not least, I would like to thank the Honors and McNair programs for providing their support throughout my academic career at Syracuse University.

Chapter 1: State of Nanotechnology

Through the past few decades, there have been great advances in technology and electronics. Previously telephones were bulky and could only be used at home, but now telephones are mobile and are smaller than the palm of your hand. Nanowires and nanotransistors that could greatly improve the mobility and efficiency of electronic devices exist separately, however there is no practical method of connecting these two nano-components. The Sponsler group is attempting to build a molecular wire that will achieve this goal. Thus new technology can be used in computers and other current electronics. The technology will not only improve the performance of current devices, but also allow for the development of new technologies such as medical devices that have sensors that can regulate hormones in the body.

There are two approaches to nanofabrication called the top-down and the bottom-up approach. The top-down approach utilizes physical processes such as chemical etching and photolithography to fabricate small devices from a bulk material.[1] In the bottom-up approach, chemical reactions are utilized to create miniscule features and compounds used in electronics.[1] In contrast to the top-down approach, one builds up from the molecule or nanostructure to the macrostructure in the bottom-up approach. The top-down approach is expensive, requires rigorous conditions and facilities, and is limited in the range of applications.[1] In the bottom-up approach, it has the potential to be cheaper, simpler to use,

applicable to a wider range of uses, and produce structures with smaller dimensions than top-down approaches.[1] The points addressed make the bottom-up approach more attractive and the choice of fabrication in this project.

Chapter 2: General Template for Design of CMCs

The design of a connectable molecular component (CMC) is shown in Figure 1, where two ruthenium metal centers are bridged by a conjugated, organic backbone. The ruthenium atoms will be coordinated with different ligands of interest, depending on the system requirements. Thus, the ligands can serve to link the single molecule to outside connections such as electrodes. In addition, the properties of the complex can be altered for the purposes of the project by coordinating different ligands to the metal centers.

Figure 1- General Structure of the CMC

Multiple reasons exist for the choice of the metal centers to be ruthenium. The group was previously successful in synthesizing a similar complex using iron (Fe).[2] Ruthenium and iron belong to the same family. Elements in the same family have the same number of valence electrons therefore, they have similar properties. In addition, ruthenium has multiple

oxidation states, has good functional group tolerance, and is selective for olefins over other functional groups.[3]

Metal complexes can adopt a wide range of geometries such as tetrahedral, square planar, octahedral etc. In the case of ruthenium, the complexes are stable as 5-coordinate and 6-coordinate complexes in the trigonal bipyramidal, square pyramidal, and octahedral geometry. Many of the ruthenium complexes are stable in the 5-coordinate or 6-coordinate arrangement because the complexes can obtain an 18-electron count. From ligand field theory, the 18-electron count is stable because many of the low energy bonding molecular orbitals are filled. Ruthenium does not obey the octet rule because it has a large atomic radius and it has 4d subshells that can accommodate the excess electrons.

Lastly, a conjugated, organic backbone is desirable because conjugation enhances electron mobility. An organic backbone also yields interesting properties such as flexibility. With this information in mind, the first of a series of methods are presented.

Chapter 3: Grubbs Catalyst and OMMI

3.1 Background and Application in Project

The first approach involves the use of a class of compounds called Grubbs catalysts and the olefin metathesis for metal incorporation (OMMI) reaction. Grubbs 1st generation catalyst was discovered in 1996 by Dr. Robert H. Grubbs and he was eventually awarded the Nobel Prize in 2005

for his entire body of work including the catalysts.[3] The 1st generation catalyst has the formula $(PCy_3)_2Cl_2Ru{=}CHPh$ and the 2nd generation catalyst has the formula $(PCy_3)Cl_2(NHC)Ru{=}CHPh$ where Cy is cyclohexyl, and NHC is an N-heterocyclic carbene. These catalysts are important for their ability to facilitate olefin metathesis. Olefin metathesis is a reaction that allows for creating new carbon-carbon bonds, reactions that are limited in organic chemistry. The catalysts are more stable and more reactive than earlier catalysts and help facilitate a multitude of reactions.[3] The catalysts have a ruthenium metal center coordinated by different ligands that can be manipulated to alter properties such as reactivity, selectivity, and stability.

Olefin metathesis for metal incorporation (OMMI) is facilitated by Grubbs catalysts. Olefin metathesis involves the swapping of alkylidene groups between two organic compounds. In OMMI, the same is true except it is used to functionalize a ruthenium metal center (Figure 2).[4] The alkylidene group $=CHR^1$ replaces the original alkylidene group coordinated to the metal center through a [2+2] cycloaddition followed by

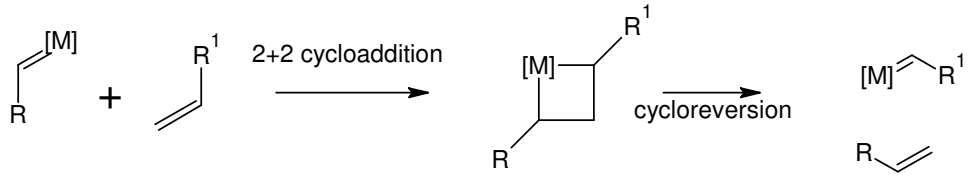

Figure 2- Olefin Metathesis for Metal Incorporation[4]

a cycloreversion reaction. It will be the reaction used to join two ruthenium metal centers together by using a conjugated organic compound with terminal double bonds (Figure 3).

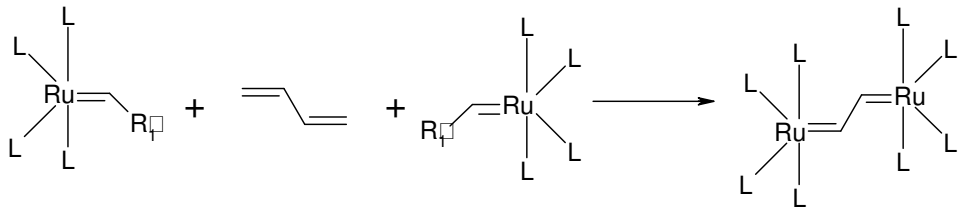

Figure 3- General Reaction Scheme of OMMI

In olefin metathesis, Grubbs catalysts are used, as its name suggests, as catalysts. In this project, the "catalysts" serve as reactants. Different variants of Grubbs catalysts can be synthesized through ligand addition or ligand substitution reactions. Aurophilic ligands coordinated to ruthenium are desired. Aurophilic means gold-loving and aurophilic ligands contain lone pairs that can bond to gold. Aurophilicity is needed in single molecule conductivity studies because the probes used for the measurements are made of gold.[5] Data can only be obtained if there is binding between the substrate and the gold probes. Following synthesis of the desired Grubbs catalysts, OMMI can be used to synthesize the diruthenium complexes as long as the stoichiometry is controlled. In the reaction, two metathesis reactions should occur at the terminals of the incoming alkene to link the ruthenium centers together.

3.2 Experimental Methods

General: Reactions were conducted in an inert atmosphere of nitrogen and at room temperature unless stated otherwise. NMR was taken

using C_6D_6 and a 300 MHz Bruker spectrometer. UV-Vis studies were conducted with a Cary50 spectrometer from 1100 nm – 190 nm using CH_2Cl_2 as solvent. CV was conducted with a model CV-27 voltammogram by Bioanalytical Systems. This project was conducted with Danielle Sherwood's assistance.

Reaction 1:

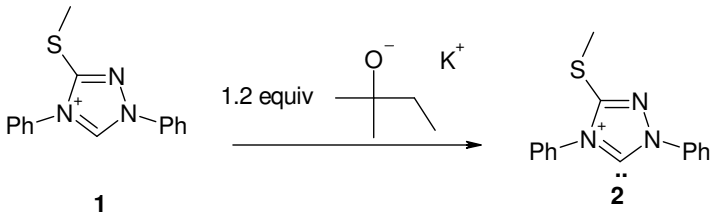

1 **2**

Preparation of Carbene (2): To a vial was added 10 mg (0.029 mmol, 1 equiv) of methylthio-1,4-diphenyl-1Hh-1,2,4-triazolium bromide and 4.34 mg (0.0344 mmol, 1.2 equiv) potassium *tert*-amyloxide in benzene. The solution was allowed to stir for an hour.

Reaction 2:

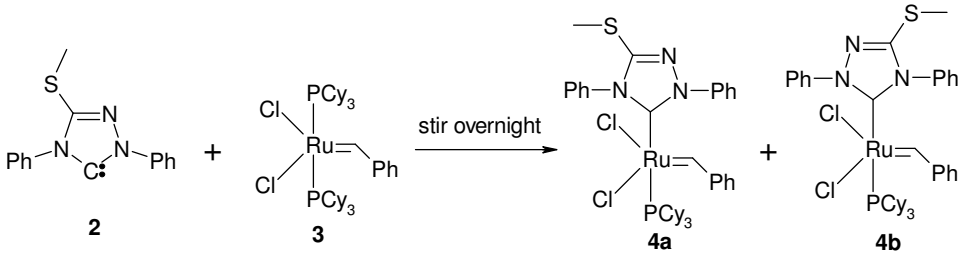

2 **3** **4a** **4b**

Synthesis of Grubbs Second-Generation Analogue (4): To 10 mg (0.029 mmol, 1 equiv) of **2** in benzene was added 23.7 mg (0.0293

mmol, 1 equiv) of Grubbs 1st generation catalyst, **3**. Before the addition of **3**, the solution was purple and after addition, the solution turned brown. The reaction was allowed to stir overnight. NMR spectroscopy was taken the next day. UV-Vis spectroscopy was conducted on solutions of **4** at $2.5x10^{-4}$ M, $1.25x10^{-4}$ M and $5.0x10^{-8}$ M. CV was also conducted on a solution of **4** at $5.5x10^{-4}$ M but no value information was obtained. Solid State IR spectroscopy was also conducted on **4** ^{1}H NMR: δ 19.80 (dd, Ru=CH), 19.94 (dd, Ru=CH), 8.1 (d, PCy_3), 2.0 (m, PCy_3). UV-Vis (λ_{max}): 321 nm, ε = 7643 $M^{-1}cm^{-1}$.

Reaction 3:

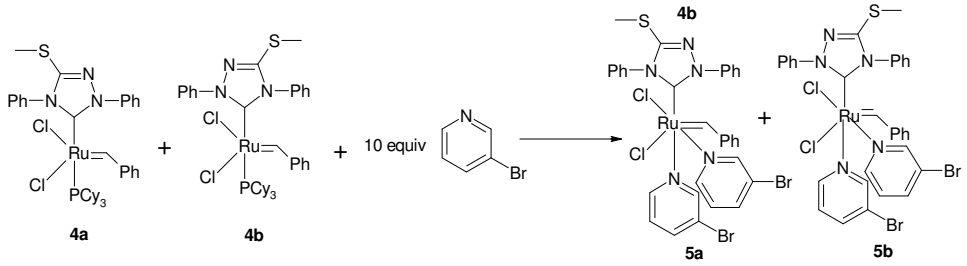

Synthesis of Grubbs Second Gen. Analogue (5): To the solution of **4** in benzene from reaction 2 was added 45.4 mg (0.287 mmol, 10 equiv) of 3-bromopyridine and stirred. Later an additional 24.4 mg of 3-bromopyridine was added. NMR spectroscopy of the solution was taken. The next day, the solvent was removed using the vac-line and the product was washed with cold pentane. NMR was taken. ^{1}H NMR: δ 19.89 (dd, 1H, Ru=CH), 19.48 (s, 1H, Ru=CH).

Reaction 4:

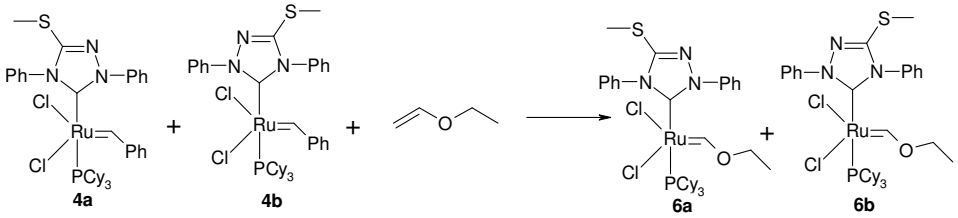

Test for OMMI Activity: To a 10 mg (0.012 mmol, 1 equiv) solution of **4** in C_6D_6 was added 0.886 mg (0.0123 mmol, 1 equiv) of ethyl vinyl ether. The solution was allowed to stir over a 48-h period while NMR was taken after 2 h, 21 h and 43 h since the start of the reaction. The color of the solution was brown. ^{1}H NMR: δ 20.0-19.8 (m, Ru=CH), 14.1 (s), 14.2 (s), 14.3 (s), 14.4 (d), 14.6 (d).

Reaction 5:

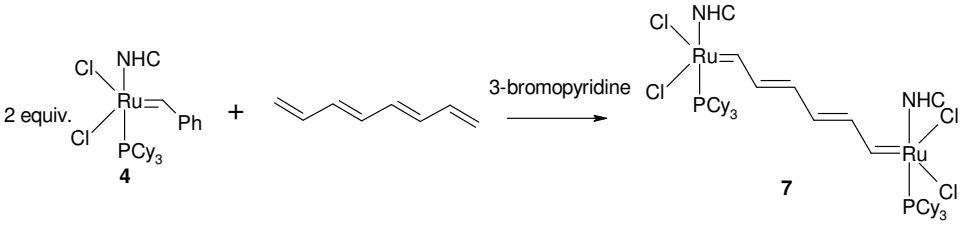

Synthesis of diruthenium complex (7): A 2:1 stoichiometry was utilized for the OMMI reaction. To 7 mg (0.009 mmol, 2 equiv) of **4** was added 0.46 mg (0.0043 mmol, 1 equiv) of octatetraene. A small amount of 3-bromopyridine was added as a catalyst. The reaction was allowed to stir and NMR was taken at different time intervals. ^{1}H NMR: δ 20-19.8 (m, Ru=CH), 19.41 (s), 19.38 (s).

3.3- Results and Discussion

From the NMR of reaction 2 (Figure 4), it can be concluded that the products of the reaction are atropisomers (**4a** and **4b**). The appearance of atropisomers with this unsymmetrical NHC is not surprising, given that slow Ru-NHC rotation is also indicated from the spectrum of Grubbs 2nd generation catalyst. The chemical shift for the alpha hydrogen with a ruthenium metal center is around 20 ppm and usually a singlet. The presence of stereoisomers explains why there are two signals at 19.89 ppm. The reason why the signals are doublets instead of singlets is that there is long-range coupling with phosphorus from the PCy_3 ligand. The UV-Vis and IR for this product are given in the appendix.

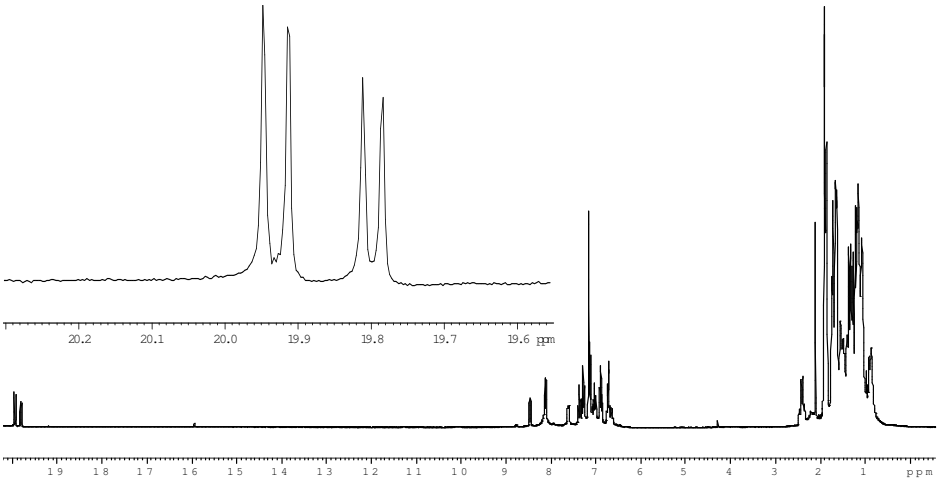

Figure 4- ^{1}H NMR of stereoisomers of products 4(a) and 4(b)

In reaction 3, 3-bromopyridine was added to increase the reactivity of the complex. Based on the NMR (Figure 5), it was observed that the reaction was not complete since the reactant peaks were still present. It was interesting to note that the signal for the product, **5,** is actually a

singlet instead of a doublet of doublets. The reason why the signal is a singlet as opposed to a doublet is because the PCy_3 ligand was substituted by 3-bromopyridine. The 3-bromopyridine ligand is substantially smaller than PCy_3 and it allows free rotation of the Ru-NHC bond. Another factor is that coordination by two 3-bromopyridine ligands gives a six-coordinate complex. Compared to the 5-coordinate complex of **4**, the NHC aryl group can fall into the vacant coordination site so that the free rotation of the Ru-NHC bond is limited. With two 3-bromopyridine ligands, there is no vacant coordinate site for the NHC aryl group to fall into therefore there is free rotation. The NMR time scale is not fine enough to resolve the rotation therefore the stereoisomers are recognized as one product.

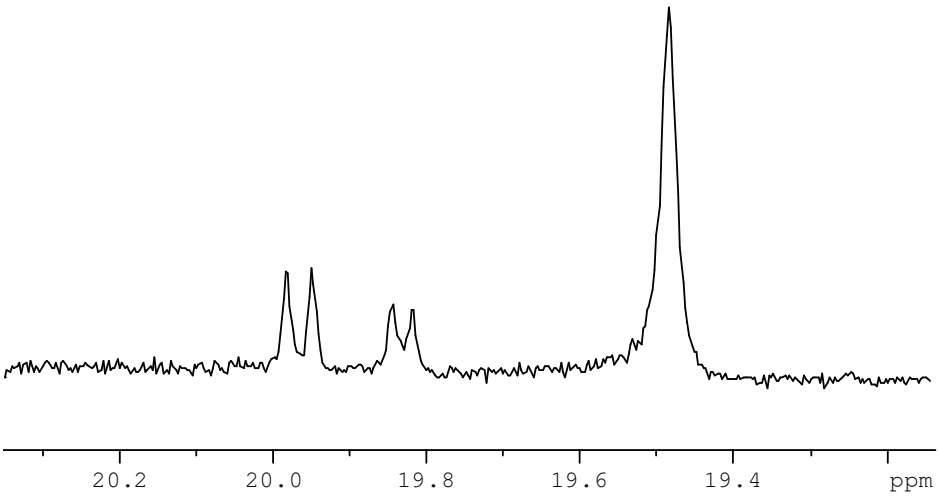

Figure 5- NMR spectroscopy illustrating results of reaction 3

Reaction 4 was conducted to determine the activity of **4** by using ethyl vinyl ether as a reactant. It was determined that **4** was metathesis active, however olefin metathesis proceeded slowly. Due to the slow reaction kinetics, 3-bromopyridine was added as a catalyst in reaction 5. In

all the metathesis reactions, products were obtained but decomposition was often the problem. The signals for products would continue to increase but within a few days, there would be no significant signals present (Figure 6).

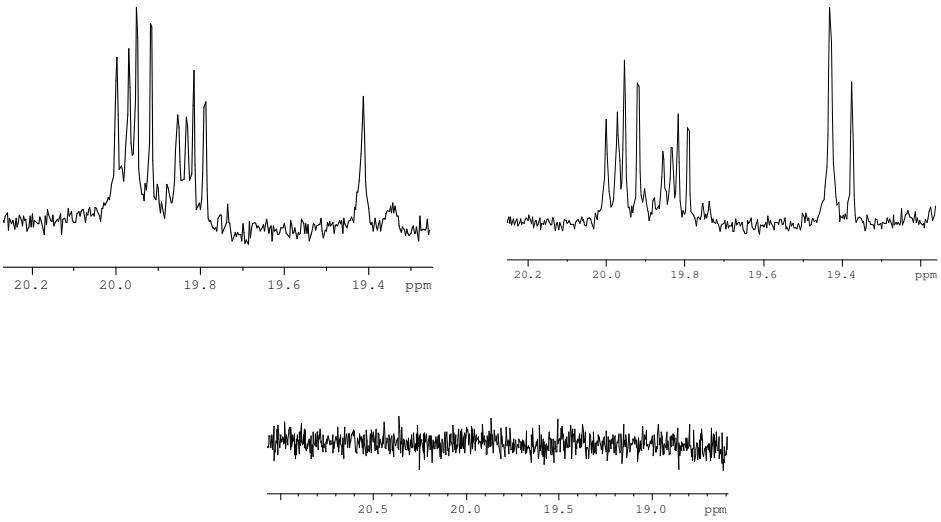

Figure 6- NMR spectroscopy showing the decomposition of products in reaction 5 after 1 h, 26 h, and 72 h respectively

Chapter 4- Hydride Insertion Reactions and Ab-Initio Studies

4.1 – Background Information

The previous method of using Grubbs catalysts as reagents in OMMI yielded limited results with our aurophilic ligand. Many of the

products were susceptible to decomposition over time as supported by NMR spectroscopy. Metal hydride insertion reactions can also be used to synthesize mono- and diruthenium complexes. The reaction between a terminal alkyne with a metal hydride results in the analogous metal vinyl complex (Figure 7). The diruthenium complex can be synthesized by using a dialkyne and two equivalents of the metal hydride.

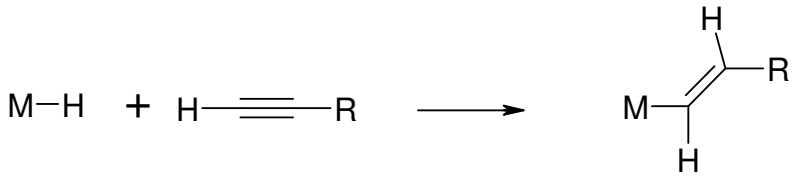

Figure 7- Generic reaction illustrating the metal hydride insertion reaction

4.2- Experimental Section

General: Reactions were conducted in air and under ambient conditions unless stated otherwise. Compound **8** was previously synthesized by Danielle Sherwood. All reagents were available in the lab and reactions were conducted at a 1:1 stoichiometry unless stated otherwise. The procedures were based on literature reactions using similar reactants.[6] NMR spectroscopy was conducted with a 300 MHz Bruker spectrometer using $CDCl_3$ as the solvent unless indicated otherwise. Solid state IR spectroscopy was conducted using a MIDAC spectrometer from Dr. Freedman's and Dr. Nafie's laboratory. UV-Vis studies were conducted using a Cary50 spectrometer from 1100 nm-190 nm at a scan rate of 600 nm/min from Dr. Hudson's laboratory. UV-Vis/NIR studies were conducted using a PerkinElmer UV Lambda 900 spectrometer from

Dr. Asefa's laboratory. Lastly, CV was conducted using a model CV-27 voltammogram by Bioanalytical Systems.

Reaction 6:

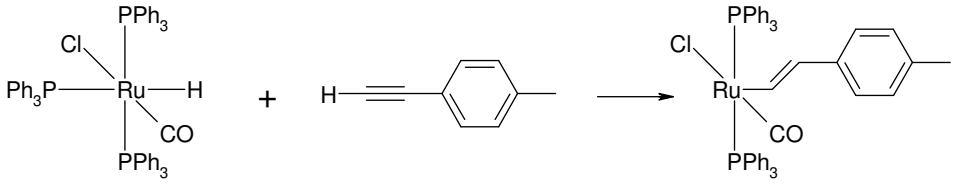

8 **9**

Synthesis of ruthenium vinyltoluene (9): To 4-ethynyltoluene (26 μL, 0.21 mmol) was added 194.2 mg (0.2039 mmol, 1 equiv) of the ruthenium hydride, **8**, in a 25 mL round bottom flask. CH_2Cl_2 (8 mL) was added and the dark red solution was stirred for 15 min. The volume was reduced to 1 mL under vacuum. Diethyl ether (19 mL) was added to obtain a cloudy red solution. The solution was placed into a freezer for 15 min for crystallization and the product was vacuum filtered and washed with ether and hexanes. The solids were rod-shaped and NMR was taken. The filtrate was placed into the freezer and more solids precipitated. The solids were isolated and washed. The yield was 43% (71 mg). The entire reaction was repeated once more. The solids were brown and the yield was 76% (140 mg). ^{1}H NMR: δ 8.35 (d, 1H, J = 12.7 Hz, Ru-CH), 7.2-7.7 (m, 30H, $2PPh_3$), 6.96 (d, 2H, J = 7.2 Hz, C_6H_4), 6.71 (d, 2H, J = 7.9 Hz, C_6H_4), 5.5 (d, 1H, J = 13.1 Hz, C=CH). UV-Vis spectroscopy was conducted on **8** (0.0013 M) and **9** ($7.0x10^{-4}$ M). Solid state IR was also conducted on **8** and **9**.

Reaction 7:

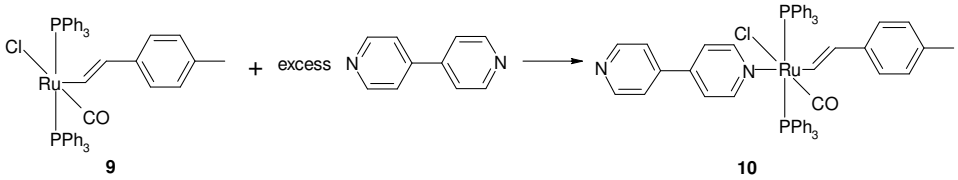

Synthesis of mono-ruthenium bipyridine complex (10): A solution of 295 mg (0.370 mmol, 1 equiv) of complex **9** and 87 mg (0.56 mmol, 1.5 equiv) of bipyridine in CH_2Cl_2 (15 mL) was stirred for 45 min. The solution was dark in color and stored in the freezer overnight. The volume was reduced under vacuum to 1 mL. Added to the solution was diethyl ether (15 mL) and heptane (3 mL) then the solution was vacuum filtered and washed with diethyl ether and heptane. The solid was greenish/yellow in color. The solid was dried and the yield was 61% (235.3 mg). The NMR spectrum was consistent with spectra of similar complexes, supporting successful synthesis of complex **10**.[6] Integration was limited by peak overlap caused by excess bipyridine. ^{1}H NMR δ 8.2 (d, 1H, J = 18.5 Hz, Ru=CH), 6.8-7.6 (m, 34H, C_6H_4 + 2PPh_3), 5.8 (d, 1H, J = 17.1 Hz, C=CH). UV-Vis and solid state IR spectroscopy was conducted on **10** ($2.0x10^{-4}$ M).

CV characterization of 10: The electrolyte tetrabutylammonium hexafluorophosphate (75.2 mg, 0.194 mmol) was added to 1.0 mg (0.0010 mmol) of **10** in THF (2.0 mL). The working electrode was a platinum disk electrode, the reference electrode was silver and the auxiliary was a

platinum foil electrode. The solution of **10** ($5.4x10^{-4}$ M) was scanned at room temperature and -78 ° C. Ferrocene was added as an internal standard.

AFM characterization of 10: Solutions of **10** (1 mM and 10 mM) in CH_2Cl_2 were added to two gold plates and left overnight. The gold plates were washed with CH_2Cl_2 and sent to Dr. Sampere of the Physics department for AFM studies.

Reaction 8

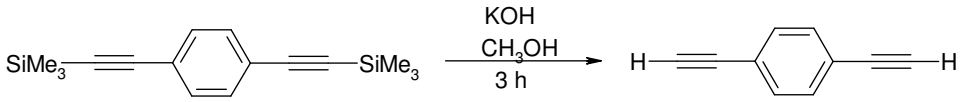

11 **12**

Synthesis of 1,4-diethynylbenzene (12): The procedure was based on literature.[7] A potassium hydroxide solution (1M) was prepared from solid potassium hydroxide and distilled water. Compound **11** (498.5 mg, 1.843 mmol) was dissolved in CH_2Cl_2 (8.33 mL) and methanol (8.33 mL). Potassium hydroxide (1 M, 3.33 mL) was added dropwise to the stirring solution. The solution changed from bright yellow to cloudy yellow and was left to stir for 3 h. The solvent was removed under vacuum and a light yellow solid was obtained. Extraction was conducted with 10 mL distilled H_2O and 3X10 mL diethyl ether. The organic layer was extracted and dried with $MgSO_4$. The organic layer was isolated and the solvent was removed. The percent yield was 77% (233.1 mg). NMR was taken and supported the synthesis of **12**.[7] ^{1}H NMR δ 7.5 (m, 4H, C_6H_4), 3.18 (s, 2H, H- C ≡ C).

Reaction 9:

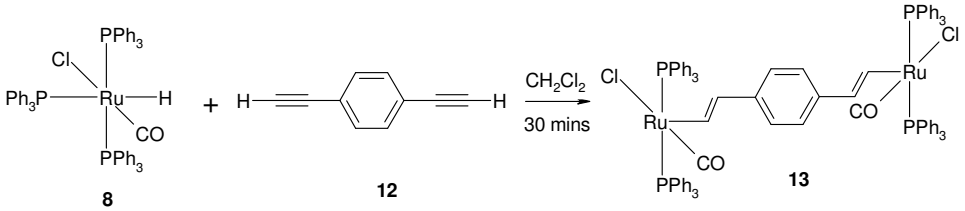

Synthesis of bis-ruthenium aryl (13): A solution of 223.4 mg (0.2346 mmol, 2 equiv) of **8** and 14.3 mg (0.114 mmol, 1 equiv) in CH_2Cl_2 (8 mL) was prepared. The red solution was stirred for 20 min then the volume reduced to 1 mL under vacuum. Diethyl ether (10 mL) and heptane (5 mL) were added to obtain a red precipitate. The solution was stored in the freezer overnight. The solution was vacuum filtered and washed with ether and heptane. The solids were reddish-brown. The solids were then dried and the yield was 70% (125.6 mg, 0.08338 mmol). NMR data supported successful synthesis.[6] ^{1}H NMR δ 8.3 (d, 2H, J = 12.6 Hz, Ru-CH), 6.9-7.9 (m, 60H, 4PPh_3), 6.6 (s, 4H, C_6H_4), 5.6 (d, 2H, J = 12.9 Hz, C=CH).

Reaction 10:

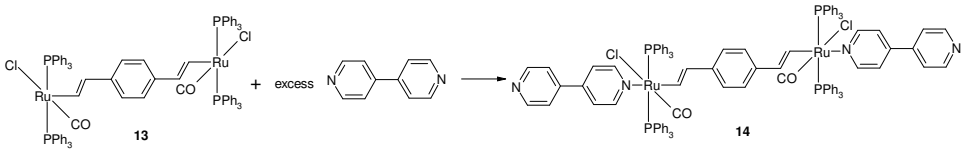

Synthesis of bis-ruthenium bipyridine complex (14): A solution of 78.7 mg (0.0522 mmol, 1 equiv) of **13** and 13.9 mg (0.0890, 1.7 equiv) of bipyridine in CH_2Cl_2 (5 mL) was prepared and stirred for 20 min. The

volume was reduced to 1 mL under vacuum and diethyl ether (10 mL) and heptane (5 mL) were added. The solution was stored in the freezer for ½ hr. then vacuum filtered and washed with ether and heptane. The solid was reddish-brown. The yield was 60% (58.3 mg, 0.0321 mmol). The solid was insoluble in $CDCl_3$, CH_2Cl_2, C_6D_6 and DMSO-d_6. An additional 15 mg (0.096 mmol, 1.8 equiv) of bipyridine was added to the solid and stirred for 40 min. and workup was repeated. NMR studies were not conducted due to the insolubility of the solid. The reaction was also tried using $CDCl_3$ as the solvent but a polymeric solid still formed.

Reaction 11:

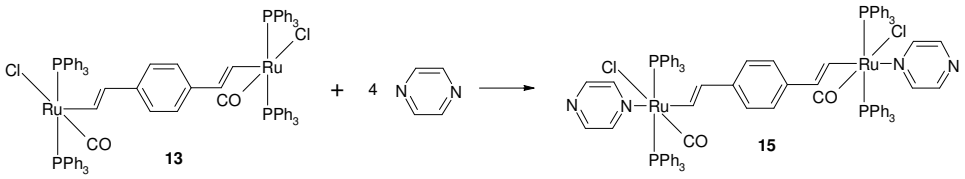

Synthesis of bis-ruthenium pyrazine complex (15): A solution of 28.2 mg (0.0187 mmol, 1 equiv) of **13** and 6.2 mg (0.077 mmol, 4 equiv) of pyrazine in CH_2Cl_2 (5 mL) was prepared and stirred. The solvent was reduced to 1 mL then ether (10 mL) and heptane (5 mL) were added. The sample was stored in the freezer and the solution was vacuum filtered and washed with ether and heptane. The solid was brown and the yield was 34% (13.6 mg). The solid was insoluble in $CDCl_3$, CH_2Cl_2 and C_6D_6 but soluble in DMSO-d_6. The NMR signals were too weak to draw any conclusions. The reaction was conducted again using $CDCl_3$ as the solvent since the starting materials were soluble in it. The NMR was taken and

supported the synthesis of **15**. ^{1}H NMR δ 6.5-7.8 (m, 64H, C_6H_4 + 4PPh_3), 5.8 (d, 1H, J = 14.7 Hz, C=CH). The peak for Ru-CH was not identified due to peak overlap.

CV characterization of bis-ruthenium aryl (13): A solution of **13** (1.7 mg, 0.0011 mmol) and tetrabutylammonium hexafluorophosphate (75.0 mg, 0.194 mmol) in THF (2.0 mL) was prepared. The solution of **13** ($5.6x10^{-4}$ M) was scanned at room temperature and at -78 ° C. A second solution of **13** ($1.0x10^{-3}$ M) was studied. Lastly, ferrocene was added to the solution.

UV-Vis/NIR Characterization of 13, 15, 15^{+}, 15^{2+}: UV-Vis spectra for **13** and **15** were obtained using Dr. Hudson's spectrometer. From a stock solution of **13** (0.001 M) was pipetted 2.4 mL (3.7 mg, $2.4x10^{-3}$ mmol, 1 equiv) of the stock and it was added to 0.9 mg (0.01 mmol, 4 equiv) of pyrazine to yield complex **15**. The spectra were taken but no conclusive results were obtained. Since UV-Vis/NIR was conducted later, the UV-Vis spectra will not be included. UV-Vis/NIR spectra were obtained using Dr. Afesa's spectrometer. A solution of **13** (2.0 mg, 0.0013 mmol) in CH_2Cl_2 (5 mL) was placed into a cuvette and flushed with nitrogen. A background scan of CH_2Cl_2 was taken prior to scans of the sample. The scan rate was 2 nm/s. Pyrazine (1.0 mg, 0.012 mmol, 10 equiv) was added to the solution of **13** then scans were taken at room temperature and -78 ° C. Ferrocenium hexafluorophosphate (0.5 mg, 0.002 mmol) was added to the solution of **15**, mixed then flushed with nitrogen. Scans were taken at room

temperature and -78 ° Celsius. A second equivalent of ferrocenium hexafluorophosphate was added and scans were taken. A scan of a standard solution of ferrocenium (4.1 mg, $3.1x10^{-3}$ M) was also taken at -78 ° Celsius.

Ab-Initio Calculations: The complexes that were compared are shown below. The complexes were also studied in the neutral, cationic and dicationic form. Complex **16** calculations were conducted previously by Sripriya Seetharaman, a former member of the Sponsler group.[8] Optimization calculations were conducted using DFT/B3LYP/lanl2dz and C_{2h} symmetry. The program cubegen was used to generate the frontier molecular orbitals diagrams.

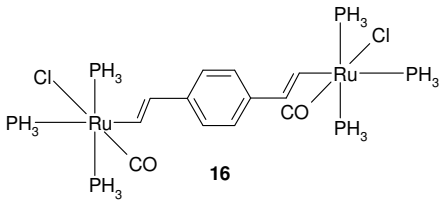

16

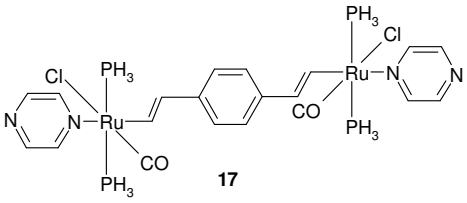

17

4.3- Results and Discussion

In the analysis of the NMR spectra pertaining to the alkenyl complexes studied, there are three characteristics peaks to identify. The first peak is a doublet around 8.5 ppm due to the alpha hydrogen, the second is around 6.0-7.0 ppm due to the aromatic C_6H_4 groups, and last is the beta hydrogen doublet around 5.5 ppm. NMR is often used to monitor the progress of a reaction and for identification. Peaks changes and shifting indicates that a reaction is occurring. Unfortunately, solubility was

a problem for the bis-ruthenium complexes and it limited the effectiveness of NMR spectroscopy. When **13** and bipyridine was added in a 1:1 ratio, an insoluble polymer was formed. The same occurred with pyrazine, which is not surprising given their similar structures and properties. A polymer is limiting in that it restricts the effectiveness and the quantity of characterizations that can be conducted, in addition, the goal of the project is to synthesize a single molecule. To solve this problem, excess ligand was used in the belief that the extra ligands will compete for coordination sites and break up the polymer. The method was not effective however. The solids for supposedly **14** and **15** were insoluble in CH_2Cl_2, $CHCl_3$, DMSO-d_6, C_6H_6 and CH_3OH. The starting materials were soluble in $CHCl_3$ so the reactions were repeated using $CDCl_3$ as the solvent. This strategy was not useful for complex **14**, but it helped in complex **15** and NMR spectroscopy supported the formation of **15**.

UV-Vis data provides information about the electronic structure of complexes. The UV-Vis spectra of mono-ruthenium complexes **8**, **9**, and **10** indicate d-d orbital transitions (appendix). A summary of the IR and UV-Vis data for **8**, **9**, and **10** is presented in Table 1. The molar extinction coefficients, ε, were calculated using Beer's law. The peak at 493 nm for **9** falls in the range for d-d type transitions, which is about 500-600 nm, and the extinction coefficient is within the expected range as well.[9] The IR peaks corresponding to carbonyl stretches were also in agreement with data of similar complexes.[10]

Table 1- IR and UV-Vis spectroscopic results

	IR:		UV-VIS		
	Stretch:	λ (nm):	Concentration (M):	λ_{max} (nm):	ε ($M^{-1}cm^{-1}$):
8	CO	1924.6	0.0013	635	330
9	CO	1927.5	0.00070	493	840
10	CO	1923.6	0.00020	411	4600

From the data, it can be observed that there is a decrease in λ_{max} going from **8** to **9** to **10**. The ruthenium center has an octahedral geometry and based on ligand field theory, the frontier molecular orbitals should consist of 3 degenerate lower energy t_{2g} orbitals and 2 degenerate higher energy e_g orbitals. There are 6 electrons that fully occupy the t_{2g} orbitals and when an electron is promoted from the t_{2g} orbital to the e_g orbital it is called a d-d type transition. Upon coordination of bipyridine to **9** to form **10**, there is an increase in electron density. The increase in electron density increases the electron repulsion experienced by the e_g orbitals, which increases the e_g to t_{2g} energy. The increase in e_g to t_{2g} energy is quantitatively expressed as a decrease in λ_{max}. The trend from **8** to **9** can also be attributed to an increase in electron density, but other factors must be considered due to the change in coordination number.

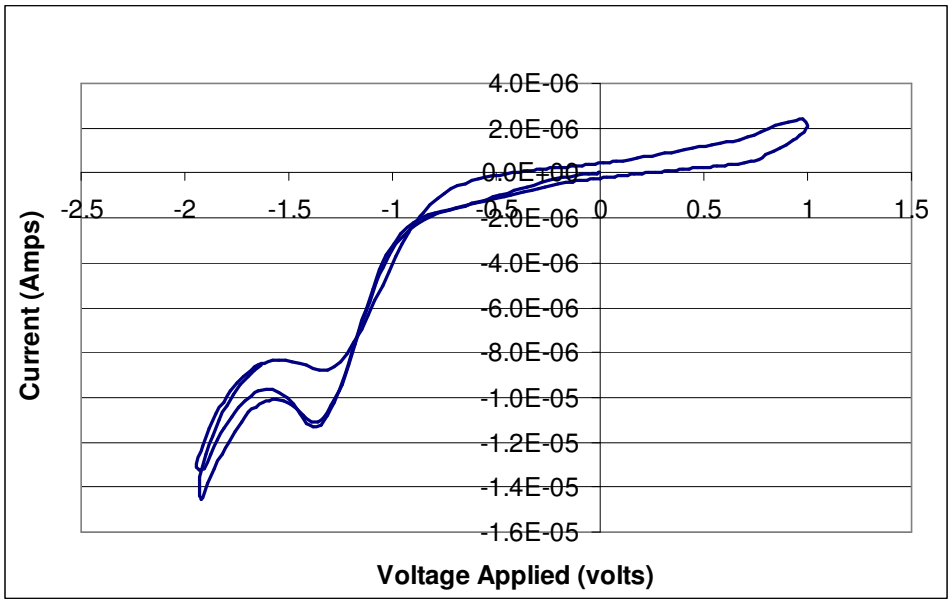

Figure 8- CV characterization of complex 10 at 0.005 mA/V; scan rate= 0.2 V/s; T = -78°C.

CV characterization conducted on **10** yielded the above voltammogram (Figure 8). A reduction wave is observed at -1.4 V but without the respective oxidation wave. For redox couples, there is usually an oxidation wave and a corresponding reduction wave. The presence of only the reduction wave shows that the process is irreversible. Changes in reaction conditions and scan parameters did not produce an oxidation wave. Side reactions or rapid decomposition of the reduced species could explain the results observed.

Further studies of **10** were conducted using atomic force microscopy (AFM). One of the uses for AFM is to obtain topographical information. In collaboration with Dr. Sampere of the physics department at Syracuse University, the graphs illustrated in Figure 9 were obtained. The AFM instrument has a gold tip that moves back and forth near the

surface of the substrate. The jagged peaks observed showed that the sample was sticky which caused the tip to drag along the surface. It is plausible since bipyridine has available lone pairs that can bond to the gold tip. Additional information regarding thickness of the substrate was obtained. By soaking the gold plates in a solution of the substrate, it was hopeful that a monolayer of **10** would deposit on the plates after drying. The ruthenium monolayer has a thickness around 20-30 Angstroms but the peaks obtained from AFM were greater than 7 µm in some cases.

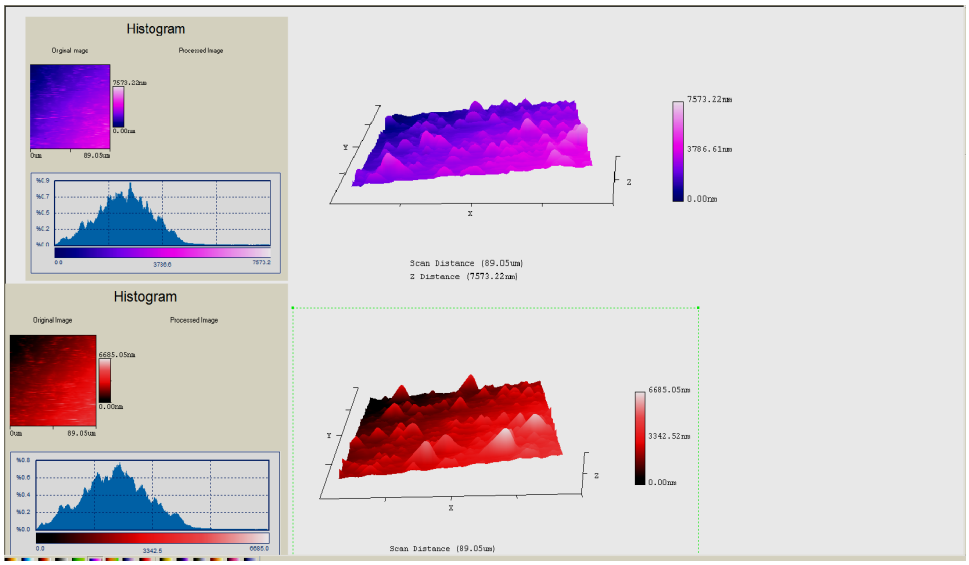

Figure 9- AFM topography of substrate 10 on gold plates; top picture is the probe going from right to left and bottom is left to right

CV characterization was conducted on complex **13** (Figure 10). There seems to be an oxidation wave around 0.33 V at a current of 0.57 µA and a reduction wave around -1.3 V at a current of -1.3 µA. The formal redox potential for the couple is -0.49 V. Previously, CV was conducted on **13** by a collaborator (Figure 11).and a comparison of the graphs show significant differences. In the later case, the redox potentials

occur at positive potentials. However, both graphs show support that the redox couple is not reversible.

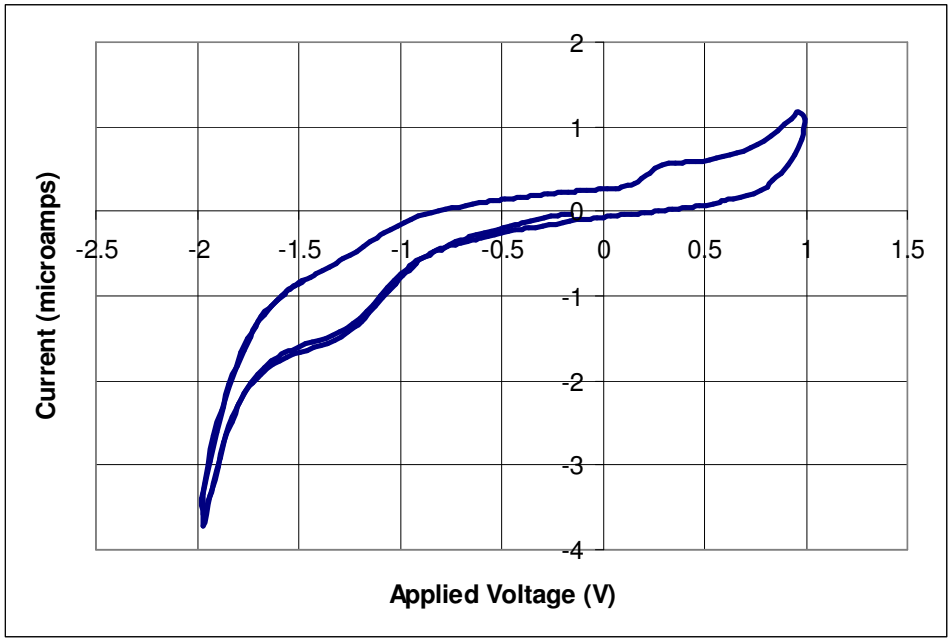

Figure 10- CV of 13 ($1.0x10^{-3}$ M) taken at -78 degrees C; scan rate: 0.20 V/s.

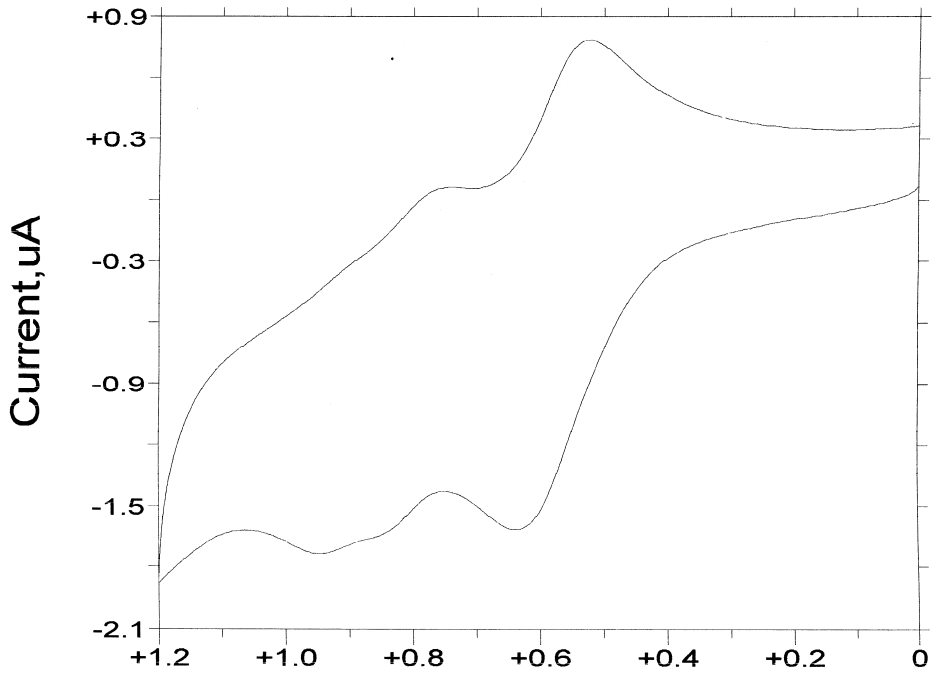

Figure 11- CV of 8 obtained previously by Casey Londergan (Kubiak group, UC San Diego)

Lastly, UV-Vis/NIR data were obtained on complexes **13**, **15**, $\mathbf{15}^{+}$, and $\mathbf{15}^{2+}$ (Table 2). The spectra were obtained in an environment of nitrogen since the cations are air sensitive. The data for **13** and the cationic species were obtained from Casey Londergan, a collaborator in the Clifford Kubiak group.

Table 2- UV/Vis-NIR results 13, 15 and cations

Compound:	λmax (nm):
13	370
$\mathbf{13}^{+}$	356, 524, 578, 1034, 1208
$\mathbf{13}^{2+}$	710
15	-
$\mathbf{15}^{+}$	528, 584, 1048, 1230
$\mathbf{15}^{2+}$	614

From the UV-Vis/NIR spectra (appendix), it appears that not enough ferrocenium was added to oxidize the monocation. The peak at 1230 nm for $\mathbf{15}^{+}$ was expected to disappear after adding a second equivalent of ferrocenium, but it did not. Therefore, the spectra were standardized and spectral subtraction was conducted to obtain the data for $\mathbf{15}^{2+}$. The data from the UV-Vis/NIR spectra indicate strong absorptions in the UV-Vis and NIR region. The signals in the UV-Vis region are due to d-d type transitions of the ruthenium center and the signals in the NIR region are due to mixed-valence π-π type transitions.[2]

There are three categories of ruthenium complexes: class I, II and III. Class I complexes have a high barrier to electron transfer, class III complexes have no electron transfer since the electrons are delocalized

and class II complexes are localized but the barrier to electron transfer is smaller than class I complexes.[11] The positive charge on **15**$^{+}$ can be localized on either one of the two ruthenium metal centers such that there are two degenerate energy levels. For class III complexes, the mixed valence state contains two ruthenium atoms each with ½ a charge. Based on the high energy of mixing between the two localized states, H_{ab}, it can be determined that **15**$^{+}$ is a class III complex.[2]

The UV-Vis/NIR data can be used to compute the numerical value of H_{ab} for class II and III complexes.[2] For class III complexes, the peak energy for the mixed-valence transition is divided by 2. The value for class III complexes often falls around 0.5 eV and the value calculated for **15**$^{+}$ is exactly 0.5 eV.[2] A rough estimation of the extinction coefficient of **15**$^{+}$ is 10,000 $M^{-1}cm^{-1}$ at 1230 nm, which is consistent with values for class III complexes. In addition, the shoulder at 1048 nm provides further evidence that **15**$^{+}$ is a class III complex.[2]

To distinguish between class II and class III complexes, Hush theory can also be used. Hush theory predicts that for class II complexes $\Delta \bar{\nu}_{1/2}$ should be equal to $(2310\,\upsilon_{max})^{1/2}$ where υ_{max} is the peak maximum in cm^{-1} and $\Delta \bar{\nu}_{1/2}$ is the width of the peak at half-height.[12] Class III complexes have peaks that are less broad than class II complexes, so if the value calculated through Hush theory is larger than the value obtained from the UV-Vis/NIR data, then **15**$^{+}$ is a class III complex. The value calculated from the UV-Vis/NIR data was 1100 cm^{-1} while the value

calculated from Hush theory was 4333 cm^{-1} providing evidence that **15**$^{+}$ is a class III complex.

Lastly, ab-initio calculations were conducted using the program Gaussian 03W. The complexes studied were **16** and **17**. Calculations on **16** and the cationic species were already conducted by Sripriya Seetharaman.[8] By comparing and analyzing the changes in the frontier molecular orbital energies, a greater understanding of the effect of pyrazine coordination can be obtained. In the analysis, only the frontier molecular orbitals with symmetry labels B(G) and A(U) were of interest because the p-orbitals are anti-symmetric with respect to the horizontal mirror plane, σ_h. For comparison, five occupied MOs for **17**, **17**$^{+}$ and 4 occupied MOs and the LUMO for **17**$^{2+}$ were used. The frontier molecular orbitals provide information regarding ruthenium d orbital interactions with the carbon chain p orbitals and electron delocalization. The frontier molecular orbital diagrams were generated using the program called cubegen and HOMO 129 for **17** is shown as an example (Figure 12).

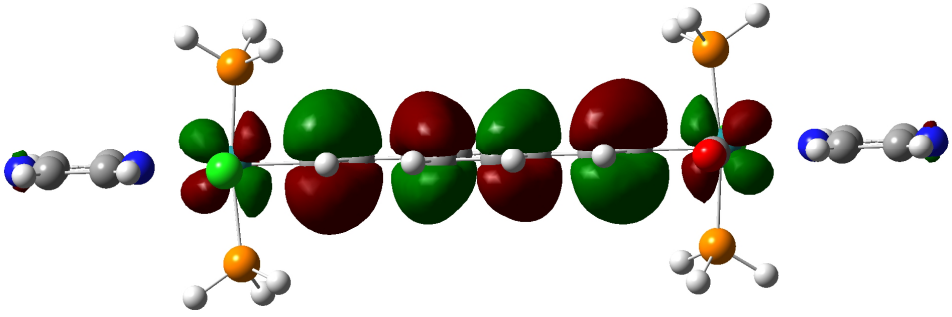

Figure 12- Example of frontier molecular orbital diagram (HOMO 129) for 17

By analyzing the interaction of the frontier molecular orbitals in **17**, the respective frontier molecular orbitals in the cation and dication were obtained. The orbital shapes, the number of nodes, delocalization and overlap were compared between the orbitals of **17** with the two cationic species. If two orbitals looked similar then they were said to represent the same molecular orbital. An example illustrating the point is that molecular orbital 129 of neutral **17** was the same molecular orbital as molecular orbital 129 of $\mathbf{17}^{+}$ (Table 3). The numbers in the table are just labels for the molecular orbitals. The "matching" process is conducted so that the changes in molecular orbital energy can be determined.

Table 3- Frontier Bridge Pi Molecular Orbital Matches for 17, 17^{+}, 17^{2+}

Neutral	+1	+2
129	129	129
128	124	
122	118	113
119	107	111
110	105	104

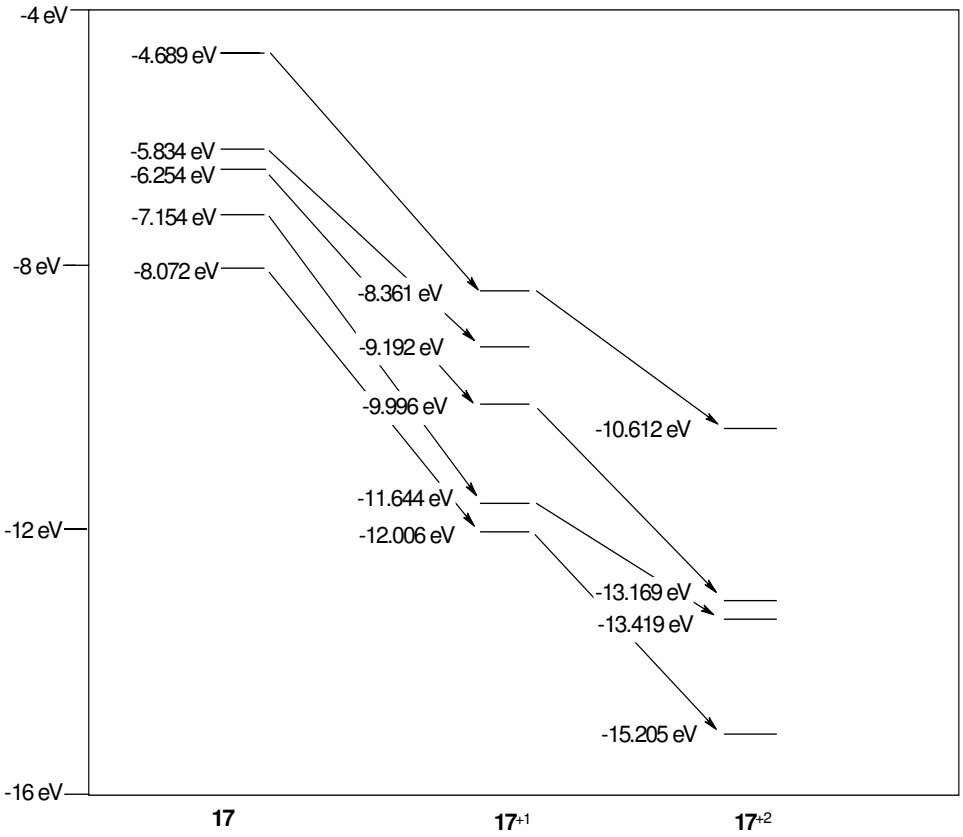

Figure 13- Frontier Molecular Orbital Energy Change Diagram for 17

After comparing the frontier molecular orbital energy diagrams, the pyrazine ligand is more able to stabilize the orbitals following oxidation than the phosphine ligand, PH_3. The molecular orbital energy of the neutral species **16** and **17** were similar but following oxidation, there were significant differences. Oxidation is the removal or loss of an electron and it decreases electron repulsion which destabilizes complexes. After oxidation, the energy of the orbitals decrease as expected from the decrease in repulsion, but the magnitude of decrease was greater for $\mathbf{17}^+$ than $\mathbf{16}^+$. For example, the energy of HOMO 129 for $\mathbf{17}^+$ and $\mathbf{16}^+$ are -8.361 eV and 6.724 eV respectively. The decrease in energy from **17** to $\mathbf{17}^+$ was 3.672 eV which was greater than the decrease of 1.937 eV

experienced from **16** to $\mathbf{16}^{+}$. The greater decrease when ruthenium is coordinated to the pyrazine ligand than the PH_3 ligand shows that pyrazine has a greater stabilizing effect following the first oxidation. In the second oxidation, the molecular orbital energies of $\mathbf{17}^{2+}$ was still lower than $\mathbf{16}^{2+}$, however the decrease in energy was greater from $\mathbf{16}^{+}$ to $\mathbf{16}^{2+}$ than from $\mathbf{17}^{+}$ to $\mathbf{17}^{2+}$. Phosphine is slightly more able to stabilize the orbitals observed from the cation to dication than pyrazine, however pyrazine provides more stabilization to the orbitals overall.

Chapter 5: Incorporation of Pincer Ligands

5.1- Background

The previous projects were limited due to solubility and decomposition problems. As an alternative to perhaps avoid the previous problems, pincer ligands were studied with central pyrazine or pyridine ligands. Pincer ligands are ligands that bind to metal centers in a meridional, multidentate fashion, and pincer ligands provide increased stability to complexes. The pyrazine and pyridine ligands studied are 2,6-bis(diphenylphosphinomethyl)pyrazine and 2,6-bis(diphenylphosphinomethyl)pyridine. The lone pairs on the phosphine and nitrogen groups are able to bind the ligands in a tridentate fashion to

the metal centers. In addition, the ligands studied are aromatic and aurophilic since the ligands have available lone pairs. Aromaticity should provide increased electron delocalization throughout the complexes which are desirable for use in CMCs and aurophilicity should help the ligands bind to gold in future single molecular conductivity studies.

5.2- Experimental Section

General: Prior to use all reaction vessels and instruments were flushed with nitrogen. Round bottom flasks and syringes were oven-dried unless stated otherwise. The ligands necessary were not available. The precursors were ordered from commercial sources and attempts were made to synthesize the desired ligands. The solvent THF was distilled and ethanol was degassed. TLC was conducted multiple times using CH_2Cl_2 to dissolve the products. NMR was taken using the Bruker 300 MHz spectrometer using solvents C_6D_6 and $CDCl_3$.

Reaction 12:

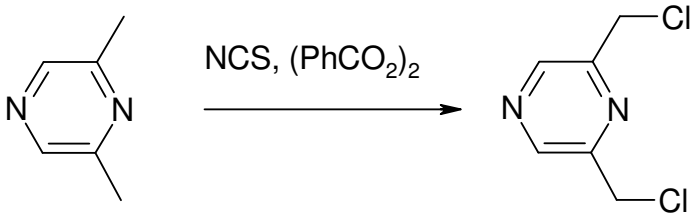

18 **19**

Synthesis of 2,6-bis(chloromethyl)pyrazine (19): Procedures were based on Eiermann et al.[13] Schlenk procedures were not observed for this reaction. A solution of 1.002 g (9.262 mmol, 1 equiv) of 2,6-

dimethylpyrazine in anhydrous THF (31 mL) was prepared in an oven-dried 50 mL round bottom flask. The round bottom was flushed with nitrogen and placed under reflux. To the solution was added 2.485 g (18.60 mmol, 2 equiv) of N-chlorosuccinimide in 4 equal portions followed by 0.0664 g (0.274 mmol) of dibenzoyl peroxide. After refluxing for 1 day, a red solution with precipitate, probably the product succinimide, was observed. After cooling the solution in an ice bath, the solvents were removed and the product washed with 2 x 10 mL CCl_4. The succinimide was vacuum filtered. After rotovapping, a yellow solid, slightly oily, was obtained. The product mass was 3.172 g while the expected yield was 1.628 g. The solid products were flushed with nitrogen then stored in the freezer. NMR was taken using $CDCl_3$ after 1 and 5 days. TLC was conducted using a 10:1 dichloromethane/ethyl acetate mixture with the product dissolved in $CHCl_3$. R_f values: 0.0, 0.19, 0.30. An attempt was also made using ethyl acetate as the mobile phase. Flash chromatography was conducted using first ethyl acetate then methanol. The reaction was conducted two more times. The third time, the reaction solvent was CCl_4. No flash chromatography was conducted for the 2nd and 3rd times.

Reaction 13 (a):

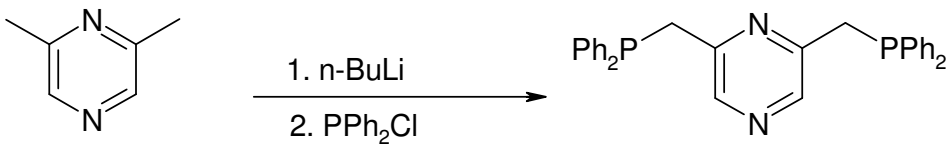

18 **20**

Titration of n-BuLi: Procedures were obtained from the literature.[14] Syringes were oven-dried and flushed with nitrogen prior to use and the solution of n-BuLi was allowed to thaw. An NMR tube was washed first with hexanes then $CHCl_3$ and acetone then oven-dried. To the NMR tube was added 0.6 mL n-BuLi then 0.1 mL of 1,5-cyclooctadiene (COD) was added and mixed. An external standard of C_6D_6 sealed in a capillary tube was added to the NMR tube. The NMR spectrum was calibrated and integrated and the concentration of n-BuLi was determined.

Synthesis of 2,6-bis(diphenylphosphinomethyl)pyrazine (20): Procedures were obtained from the literature.[15, 16] The concentration of n-BuLi used was 1 M. A solution of 0.2545 g (2.353 mmol, 1 equiv) of 2,6-dimethylpyrazine in ethyl ether (10 mL) was refluxed for a few minutes. To the solution was added dropwise 4.6 mL (4.6 mmol, 2 equiv) of n-BuLi. A red precipitate formed upon addition. The solution was refluxed for 1.5 h. Additional ethyl ether (4 mL) was added. Eventually the precipitate dissolved back into solution. After 1.5 h, 0.80 mL (4.5 mmol, 2 equiv) of chlorodiphenylphosphine was added dropwise and the solution was left to stir overnight for 15 hrs at rt. The solvent was removed using the vac-line and toluene (21 mL) was mixed with the product. Vacuum filtration and gravitational filtration was conducted to obtain a dark red filtrate that was stored overnight in the freezer. No crystals precipitated. After removing the solvent, the product was dissolved in $CDCl_3$ and an NMR was taken. Recrystallization was then attempted. While heating, a mixture of toluene,

hexane and $CHCl_3$ was added and the solution was allowed to cool to rt. No crystals precipitated so the solution was filtered using pipettes plugged with kimwipe. The filtrate was stored in the freezer and orange crystals were obtained after a few days. The crystals were vacuum filtered and washed with toluene then placed under nitrogen. NMR was taken using $CDCl_3$.

Reaction 13(b):

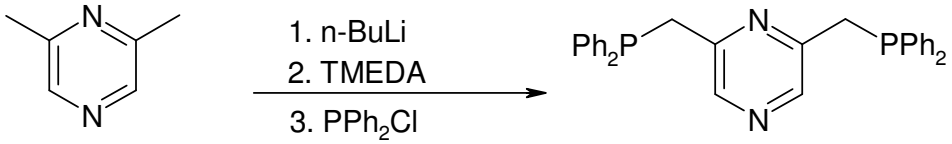

18 **20**

Synthesis of 2,6-bis(diphenylphosphymethyl)pyrazine (20):

Procedures were obtained from the literature.[15, 16] The concentration of n-BuLi used was 1.3 M. In this reaction, 0.1510 g (1.387 mmol, 1 equiv) of 2,6-dimethylpyrazine, 0.42 mL (2.8 mmol, 2 equiv) of tetramethylethylenediamine (TMEDA), 2.3 mL (3.0 mmol, 2 equiv) n-BuLi and 0.50 mL (2.8 mmol, 2 equiv) of chlorodiphenylphosphine were added in the respective order. Again, upon addition of n-BuLi, a dark red precipitate formed. The workup and procedures were the same as reaction 13(a). NMR was taken and recrystallization was attempted but no crystals were obtained.

Reaction 14:

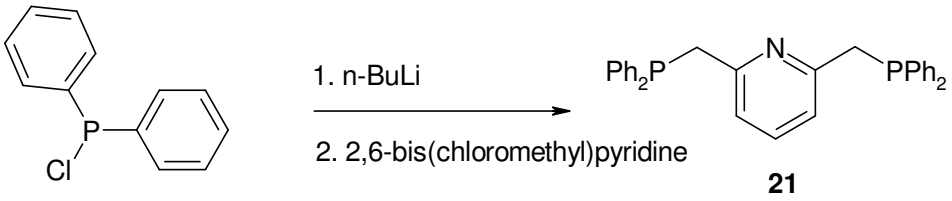

21

Synthesis of 2,6-bis((diphenylphosphino)methyl)pyridine (21):

The procedures were obtained from the literature.[17] The concentration of n-BuLi was assumed to be roughly 1 M. Using Schlenk procedures, a solution of 0.32 mL (1.7 mmol, 2 equiv) of chlorodiphenylphosphine in anhydrous THF (7mL) was prepared in an oven-dried round bottom flask. Added dropwise was 1.75 mL (1.75 mmol, 2 equiv) of n-BuLi. The solution turned from clear to yellow then to an orange color. The solution was stirred for ½ hrs in an ice bath. A solution of 0.1463 g (0.8311 mmol, 1 equiv) of 2,6-bischloromethylpyridine in anhydrous THF (6 mL) was added. Upon addition, the solution color turned to red then back to yellow. The solution was mixed for 5 h. at 0 ºC. More THF was added. Unfortunately, at one point the septum popped off. After 5 h, degassed ethanol (9 mL) was added and the solids dissolved back into solution. The solvent was removed under rotovap and an NMR was taken. Flash chromatography was conducted using a mixture of CH_2Cl_2/hexanes as the mobile phase while the product was dissolved in CH_2Cl_2. One fraction was collected then methanol was used to collect the second fraction. The solvent was removed by rotovap. The first fraction was a clear liquid while the second fraction contained two liquids. One layer was a clear

liquid and the second was a yellow oil. NMR was taken using $CDCl_3$. Both liquids appeared to be mostly miscible in $CDCl_3$.

5.3- Results and Discussion

In organic chemistry, there often exists many synthetic routes to make a desired compound and in this paper, only a few were explored to make the pincer ligands. It was difficult to obtain literature procedures to synthesize the exact ligand and the literatures that were obtained had low yields. Fortunately, the procedures for reactions 12 and 14 were for synthesizing the same ligand while the procedures for reaction 13 were for a similar ligand, so procedures and conditions such as solvents, were changed slightly.

Reaction 12 was a free radical reaction. Free radical reactions can be tricky due to selectivity and reactivity problems. In the halogenation of the pyrazine molecule, NCS was used as the source of chlorine atoms while benzoyl peroxide was the radical initiator. A potential problem is the control of the extent of the reaction e.g. monohalogentation versus dihalogenation. To address the issue of selectivity, the methyl positions should be favored over the aromatic positions since halogenation at the methyl position would preserve aromaticity. Therefore, there should be selectivity for the methyl position and to ensure that the dihalogenated product is formed, 2 equivalents of NCS were used.

From the NMR of the reaction (Figure 14), the starting material peaks for **18** are at 8.26 ppm (s, 2H) and 2.54 ppm (s, 6H).[18] Most of the starting material**, 18** reacted. The product peaks **19** are at 4.71 ppm (s, 4H) and 8.72 ppm (s, 2H).[12] However, it is somewhat difficult to conclude that the product was made. There are also contaminants present in the sample. There is the solvent, THF, and dibenzoyl peroxide as evidenced by the NMR.[18, 19] TLC was conducted to determine whether the product was synthesized. The expected R_f value was 0.55 but there were no spots with that value. The product was purified via flash chromatography and NMR was taken. There was no data supporting the formation of the desired product. It can be concluded that a reaction did occur but the product(s) was not **19**.

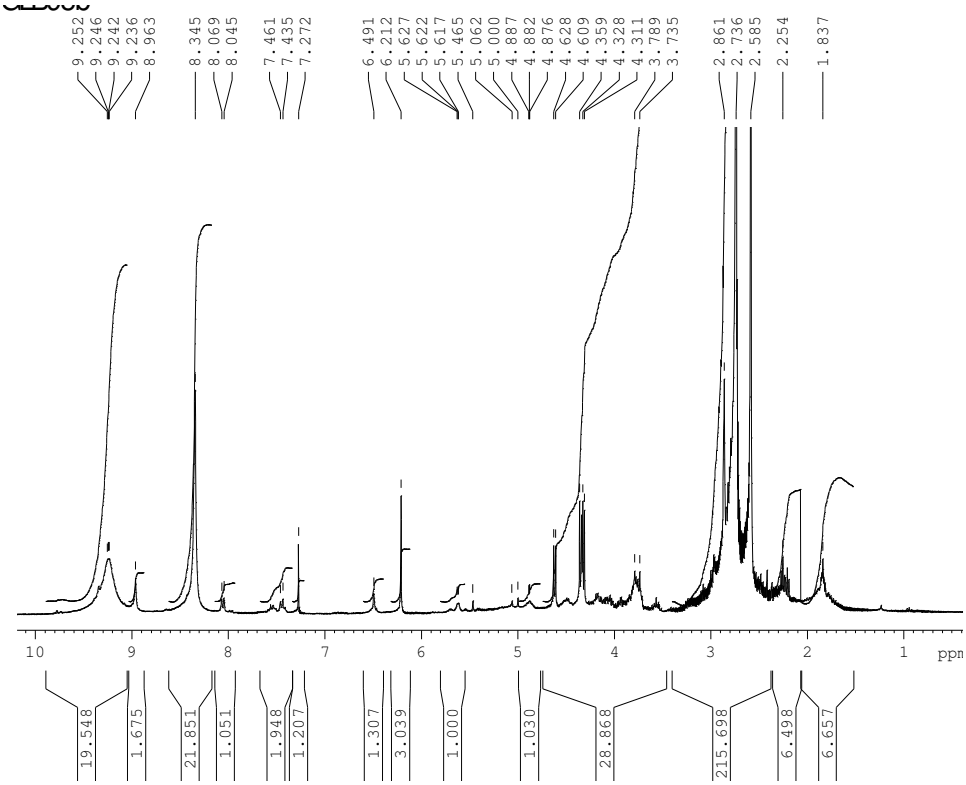

Figure 14-NMR of reaction 12

In a third attempt of reaction 12, CCl_4 was used as the reaction solvent. Similar to the prior attempts, there were impurities such as NCS and dibenzoyl peroxide present in the sample as evidenced by the NMR (Figure 15). However, there are also two peaks around 4.63 ppm and 8.65 ppm that could be the product. A TLC analysis also produced a spot with an R_f value of 0.50. The reaction might have produced the desired product but the yield is much too low. It is often a problem in free radical reactions that yield is too low due to issues with selectivity and control. If one wanted to pursue this reaction, changing the reaction conditions and

purification of the product might yield cleaner and more of the desired products.

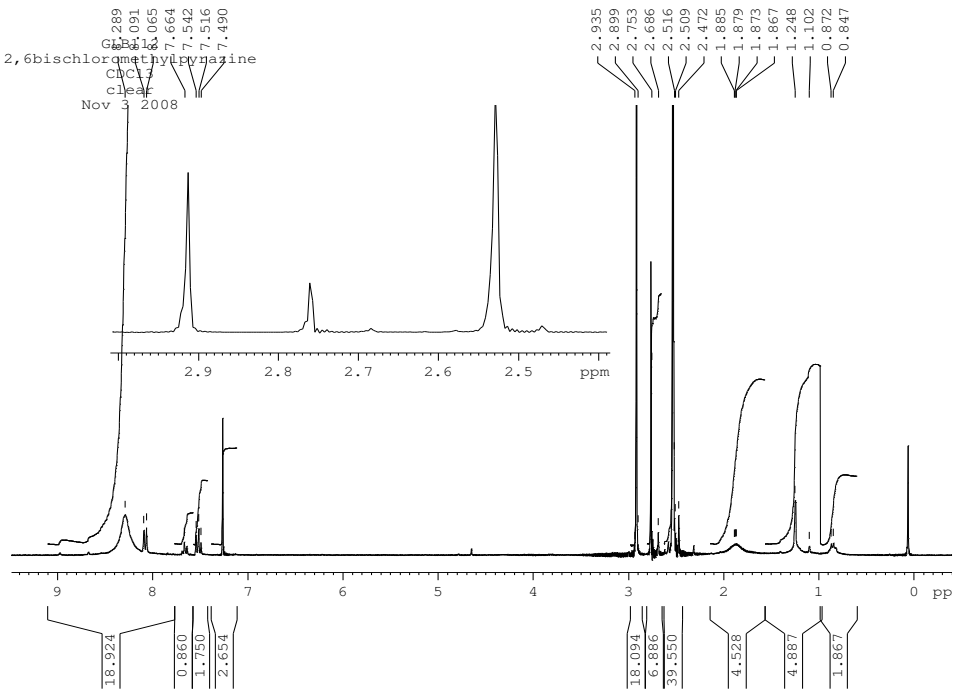

Figure 15- NMR for reaction 12 in CCl_4

The theory behind reaction 13(a) is that n-BuLi, a strong base, will deprotonate a methyl hydrogen from **18**. The **anionic 18** would displace a chlorine atom from the chlorodiphenylphosphine through a substitution reaction. A complication to the reaction is that deprotonation occurs at one of the aromatic hydrogens. It is not as likely to occur becausethe hydrogen at these positions are less basic than the methyl hydrogens. In addition, deprotonation of the methyl hydrogen is more favorable because the excess electrons can be delocalized throughout the ring to give multiple resonance structures and stabilize the anion. The NMR of the reaction (Figure 16) shows impurities of toluene and hexane. There should

be signals around 7-8 ppm for the aromatic hydrogens of the product and signals for CH_2P hydrogens around 3.25 ppm.[19] The lack of these signals indicate that the product was not successfully synthesized.

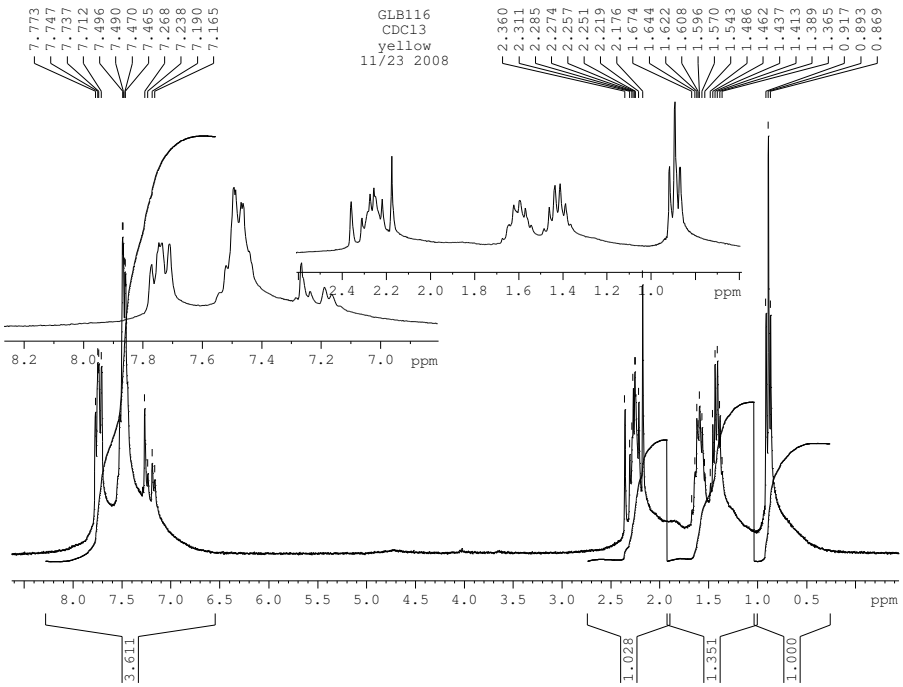

Figure 16- NMR of reaction 13(a) in $CDCl_3$

To improve upon reaction 13(a), two equivalents of TMEDA were added in reaction 13(b). TMEDA can coordinate to the lithium ion and prevent the formation of aggregates to make the n-BuLi reagent more reactive. In the reaction, there was formation of a red precipitate following the addition of n-BuLi. The precipitate could be a lithiated pyrazine complex. It explains the immediate formation of a red precipitate upon addition of n-BuLi as well as the dissolution of the precipitate as the reaction continued. The NMR of the product (Figure 17) shows impurities

of ether and toluene. The expected singlet at 3.25 ppm is also absent and indicates that the product was most likely not formed.

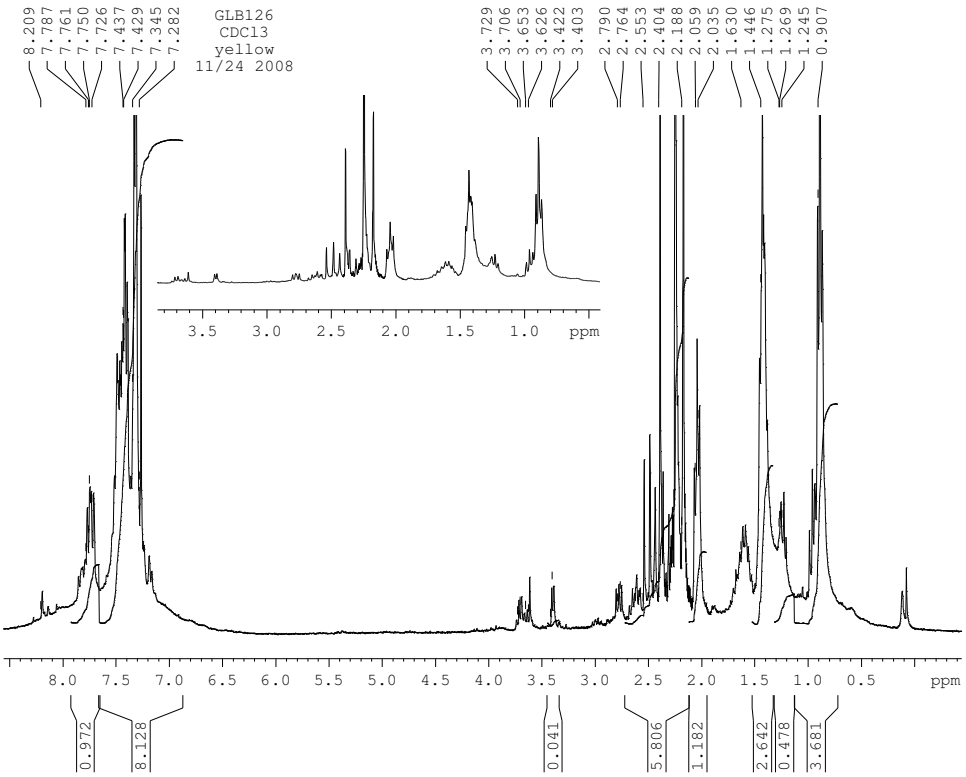

Figure 17- NMR of crude product from reaction 13(b)

Due to the limited success of the previous reactions, a different approach was taken for reaction 14. Previously in reaction 13, the nucleophile was the lithiated pyrazine, but the nucleophile in this reaction is the diphenylphosphine anion. Upon addition of n-BuLi to chlorodiphenylphosphine, the lithium chloride salt should precipitate out of solution. A substitution reaction should occur with the chlorodiphenylphosphine anion substituting for the chlorine atoms on 2,6-bis(chloromethyl)pyridine, which was purchased from commercial sources. The pyridine ligand was studied instead of the pyrazine ligand since the

previous reactions using pyrazine were not successful. Pyridine makes for a good comparison due to the similarities in structure and properties with pyrazine. If the reaction works with pyridine, it could provide insight as to the failure of the previous reactions. As noted previously, two fractions consisting of liquids were obtained after flash chromatography. The NMR of the first fraction does not contain the desired product (Figure 18). The only peak in the aromatic region belongs to $CDCl_3$. The integration and shifts of the other peaks do not belong to any of the reactants or solvents used in the system. It is difficult to assign a compound(s) as the owner of the peaks.

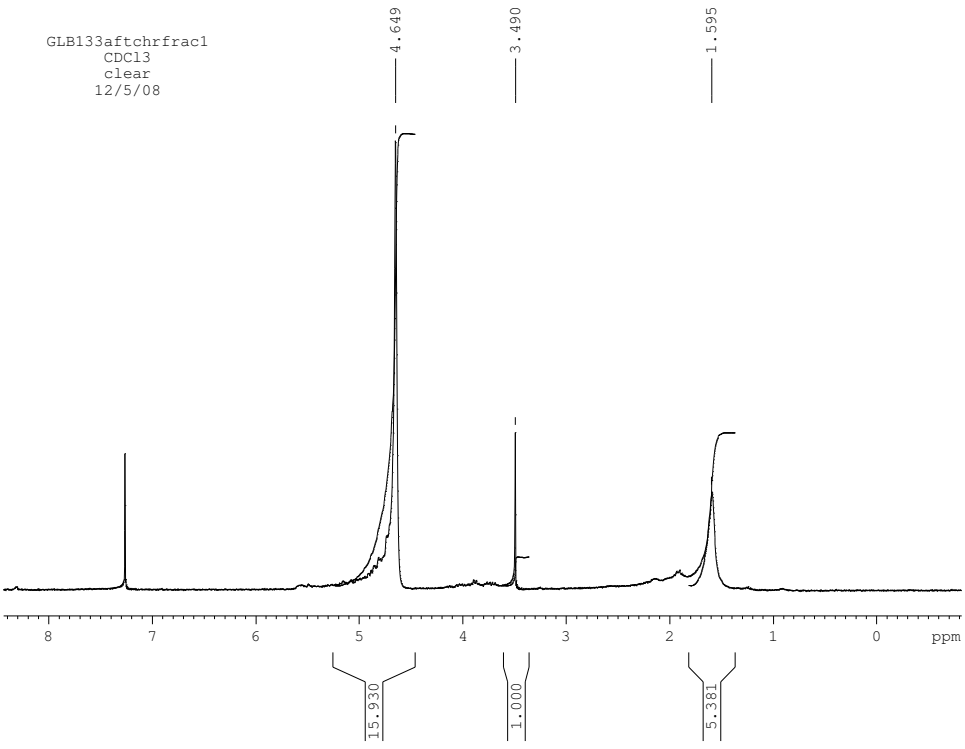

Figure 18- NMR of the first fraction following purification in reaction 14

In the second fraction, there were two layers. There was a clear and a yellow layer; an NMR of both layers were taken. The yellow layer contains many impurities such as ethanol, THF, hexanes and CH_2Cl_2. The peak at 3.48 ppm could be the hydrogens on CH_2P, but peaks in the aromatic region are difficult to assign (Figure 19). The NMR of the clear layer (Figure 20) is much more resolved. There are solvent peaks for hexane, but the identities of the other peaks are uncertain. If the desired product was successfully synthesized, it is most likely present in the yellow layer of the second fraction. As noted, the procedure was based on literature and the author reported spectroscopic data, but unfortunately the NMR data was not published. [16]

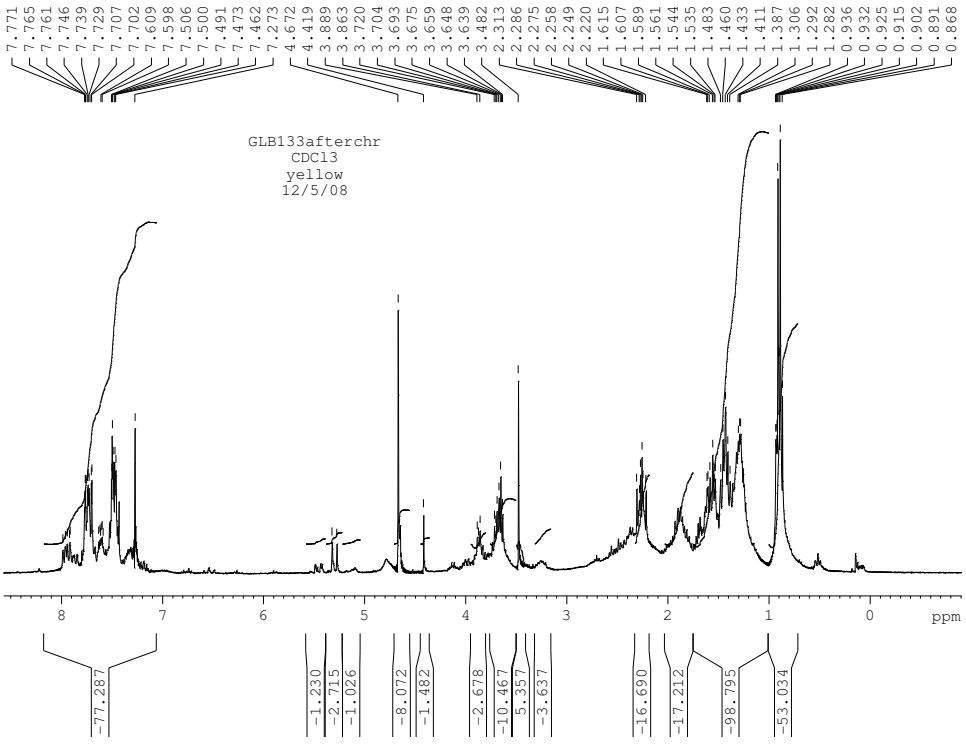

Figure 19- NMR of the yellow layer in fraction 2 of reaction 14

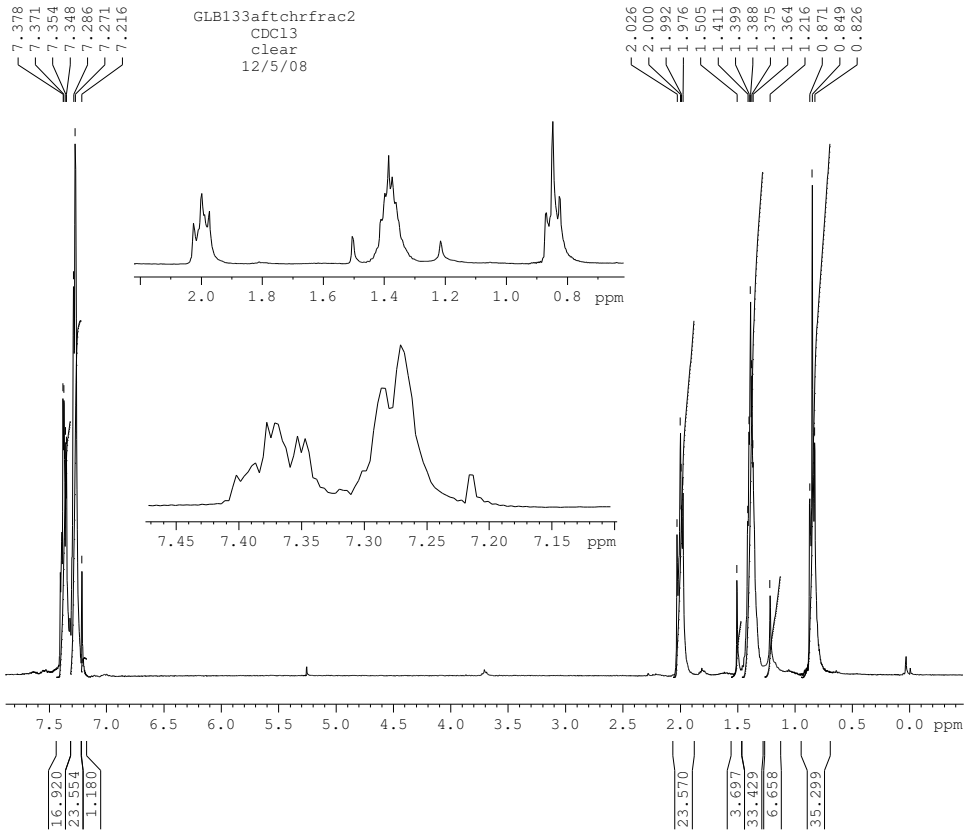

Figure 20- NMR of the clear layer in fraction 2 of reaction 14

In many reactions, the products were contaminated with impurities and recrystallization was not successful. Further projects could include purification steps or more rigorous purification steps to remove the solvents and reactants. Aside from the problem of reproducibility, the other problem was yield. In reaction 3, the author reported a 70% yield[16], however other literature procedures used and reviewed reported yields around 30% or lower. It is a goal for the future to maximize the yield.

Chapter 6: Conclusion

The aim of this thesis was to synthesize aurophilic diruthenium complexes linked by conjugated organic bridges. There is interest in practical methods of connecting nano-components and these diruthenium complexes could be a solution to the problem. The goal was to synthesize diruthenium complexes that were not only aurophilic, but exhibited stability, solubility, and electrochemical properties desirable for use as molecular wires and CMCs. A variety of chemical reactions and chemical techniques were used. The reactions used were olefin metathesis for metal incorporation, radical reactions, substitution reactions, and metal hydride insertion reactions. Some of the techniques used were chromatography, crystallization, filtration, etc. Following the successful synthesis, characterization and single molecule conductivity studies was going to be conducted.

While this project was a success, it was limited in terms of final CMC synthesis. Many of the reactions involving the monoruthenium complexes and precursors were successful, but there was trouble with the diruthenium complexes. The products of the OMMI reactions were plagued with issues of decomposition and stability. There was more success from the products of the metal hydride insertion reactions, but the major problem in this project was insolubility and that hindered the identification and characterization of the products. The last project with the pincer ligands was more in the field of organic synthesis and none of

the reactions attempted produced significant results. It was difficult to obtain high yields of the product and to identify from ^{1}H NMR whether the desired product was synthesized.

Even though many of the ideas were theoretically sound, it was unfortunate that in practice, the expected results were not obtained. It is well known that the organometallic synthesis of these classes of CMC is challenging and unpredictable. There still exist many more possible routes to make CMCs and this thesis only introduces a small percentage of the work in the field. This project provided the Sponsler group with invaluable experimental results that will guide future synthesis and serve other groups in their research. The project also increased my exposure and knowledge and provided invaluable experience in the field of chemistry that will serve me in my future endeavors.

Sources Cited and Consulted:

1. Gates, B. D.; Xu, Q.; Stewart, M.; Ryan, D.; Willson, C. G.; Whitesides, G. M. New Approaches to Nanofabrication: Molding, Printing, and Other Techniques. *Chem. Rev.* **2005,** *105*, 1171-1196.

2. Chung, M. C.; Gu X.; Etzenhouser, B. A.; Spuches, A. M.; Rye, P. T.; Seetharaman, S. K.; Rose, D.; Zubieta, J. A.; Sponsler, M. B. Intermetal Coupling in [(h5-C5R5)Fe(dppe)]2(μ-CH=CHCH=CH) and Their Dication and Monocation Mixed-Valence Forms. *Organometallics* **2003**, *22*, 3485-3494.

3. Trnka, T. M.; Grubbs, R. H. The Development of L_2X_2RuCHR Olefin Metathesis Catalysts: An Organometallic Success Story. *Acc. Chem. Res.* **2001,** *34*, 18-29.

4. Bolton, S. L.; Schuehler, D. E.; Niu, X.; Goapl, L.; Sponsler, M. B. Olefin Metathesis for Metal Incorporation: Preparation of Conjugated Ruthenium Containing Complexes and Polymers. *J. Organomet. Chem.* **2006,** *691,* 5298-5306.

5. Cui; X.D.; Primak, A.; Zarate, X.; Tomfohr, J.; Sankey, O.F.; Moore, T.A.; Gust, D.; Harris, G.; Lindsay, S.M. Reproducible Measurement of Single Molecule Conductivity. *Science* **2001,** *294*, 571-574.

6. Jia, G.; Wu, W.F.; Yeung, R.C.; Xia, H.P. Dimeric and polymeric ruthenium complexes with Ru-vinyl linkages. *J. Organomet. Chem.* **1997,** *539*, 53-59.

7. Plater, J. M.; Sinclair J. P.; Aiken, S.; Gelbrich, T.; Hursthouse M. B. The Cam lattice revisited. Gel formation from a linear bis-isocyanuric acid and 2-amino-4,6-bis-(4-*tert*-butylphenylamino)-1,3,5-triazine. *Tetrahedron*. **2004,** *60*, 6385-6394.

8. Seetharaman, Sripriya K., Ph.D. thesis, Syracuse University, 2005.

9. Maurer, J.; Linseis, M.; Sarkar, B.; Schwederski, B.; Niemeyer, M.; Kaim, W.; Zalis, S.; Anson, C.; Zabel, M. Winter, R. F. Ruthenium Complexes with Vinyl, Styryl, and Vinylpyrenyl Ligands: A Case of Non-innocence in Organometallic Chemistry. *J. Am. Chem. Soc.* **2008**, *130*, 259-268.

10. Santos, A.; Lopez, J.; Galan, A.; Gonzalez, J.J.; Tinoco, P.; Echavarren, A.M. The Effect of N-Donor Ligands on the Reaction

of Ruthenium Hydrides with 1-Alkynes. *Organometallics* **1997**, *16*, (15), 3482-3488.

11. Sonja, B. B-S.; Wiest, O. Theoretical Studies of Mixed-Valence Transition Metal Complexes for Molecular Computing. *J. Phys. Chem.* **2003**, *107*, 285-291.

12. Eiermann, U.; Krieger, C.; Neugebauer, F.A.; Staab, H.A. [2.2](2,6)- and [2.2](2,5)Pyrazinophanes: Synthesis and Molecular Structure. *Chem. Ber.* **1990**, *123*, 523-533.

13. Hoye, T.R.; Eklov, B.M.; Voloshin, M. No-D NMR Spectroscopy as a Convenient Method for Titering Organolithium (RLi), RMgX, and LDA Solutions. *Organic Letters*, **2004**, *6*(15), 2567-2570.

14. Epsztajn, J.; Bieniek, A.; Brzeinski, Z. Lithiation of Pyrido[b]cycloalkenes with Phenyllithium. *Bull. Acad. Pol. Sci., Ser. Sci. chim*. **1975**, *23*(11), 917-922.

15. Olbert, D.; Kalisch, A.; Herzer, N.; Gorls, H.; Mayer, P.; Yu, Lian; et al. Syntheses of *N*-(Diphenylphosphanyl)-2-pyridylmethylamine and Its Use as a Ligand in Magnesium and Zinc Complexes. *Z. Anorg. Allg. Chem.* **2007**, *633*, 893-902.

16. Ziessel, R. A new family of aromatic polyimine chelates substituted with two diphenylphosphines. *Tetrahedron Letters*. **1989**, *30*(4), 463-466.

17. Hush, N. S. *Prog. Inorg. Chem*. **1967,** *8*, 391-444.

18. Spectral Data Base System for Organic Compounds. http://riodb01.ibase.aist.go.jp/sdbs/cgi-bin/cre_index.cgi?lang=eng (Oct 2008).

19. Gottlieb, H.E.; Kotlyar, V.; Nudelman, A. NMR Chemical Shifts of Common Laboratory Solvents as Trace Impurities. *J. Org. Chem.* **1997,** *62*(21), 7512-7515.

Appendix:

Figure 21- IR spectrum for stereoisomers of 4

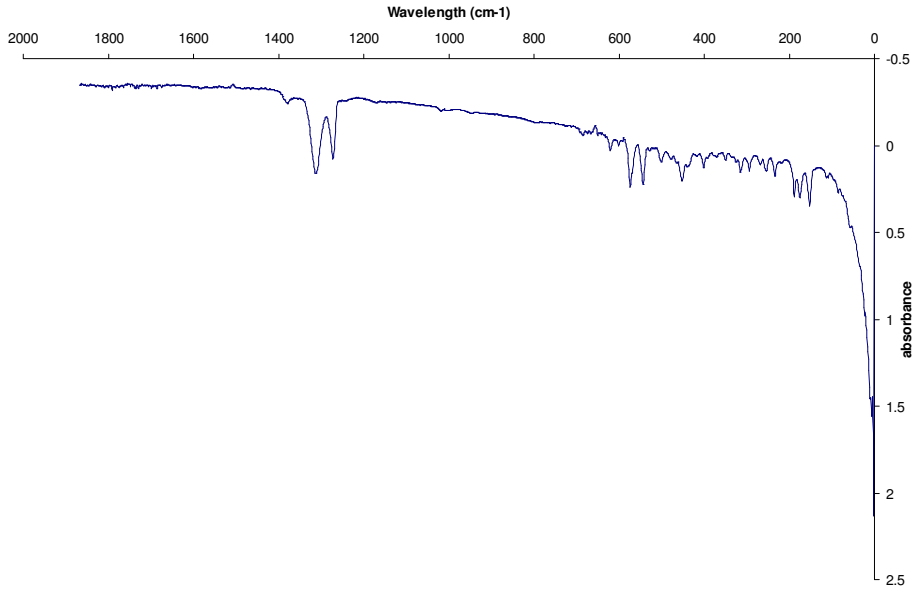

Figure 22- UV-Vis spectrum for stereoisomers of 4

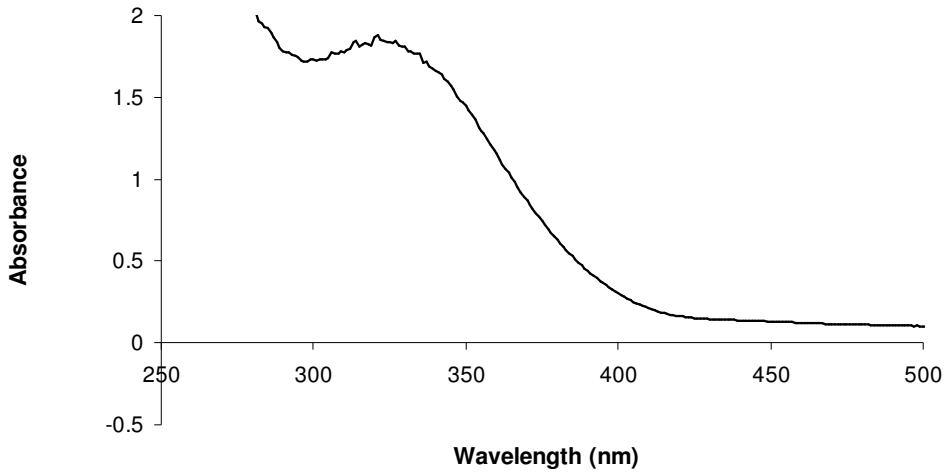

Figure 23- UV-VIS for monoruthenium complexes 8,9, and 10

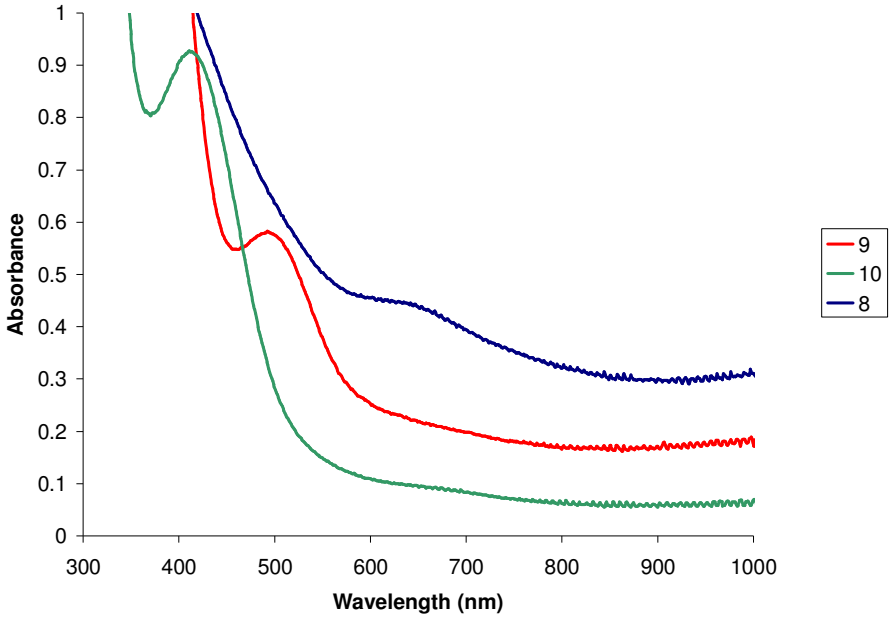

Figure 24- IR spectroscopy of monoruthenium complexes 8, 9, and 10

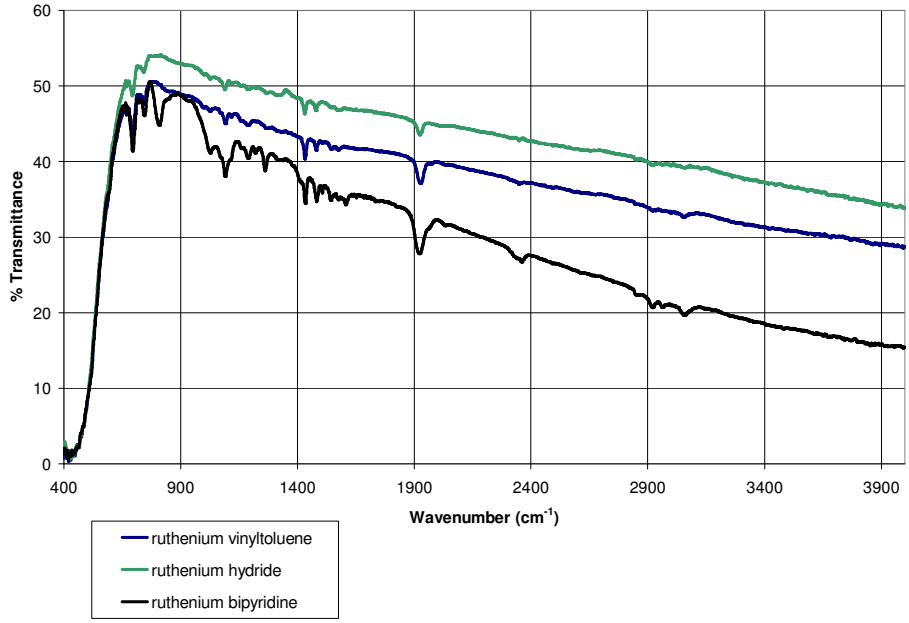

Figure 25- UV-Vis/NIR spectra for 13, 15, 15^{+}, and 15^{2+}

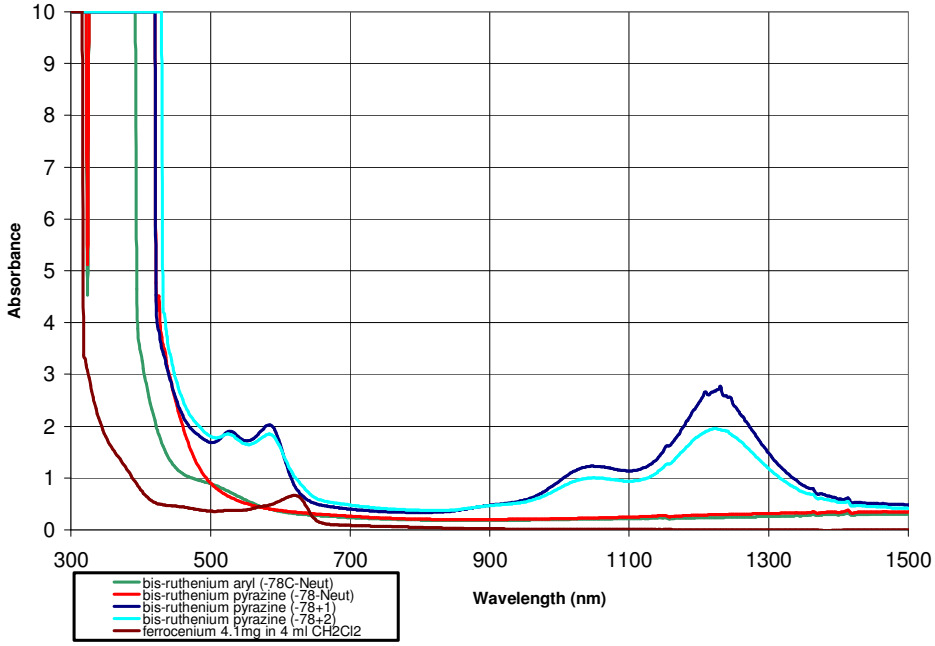

Figure 26- UV-Vis/NIR spectra for 13, 15, 15^{+}, and 15^{2+} in wavenumbers

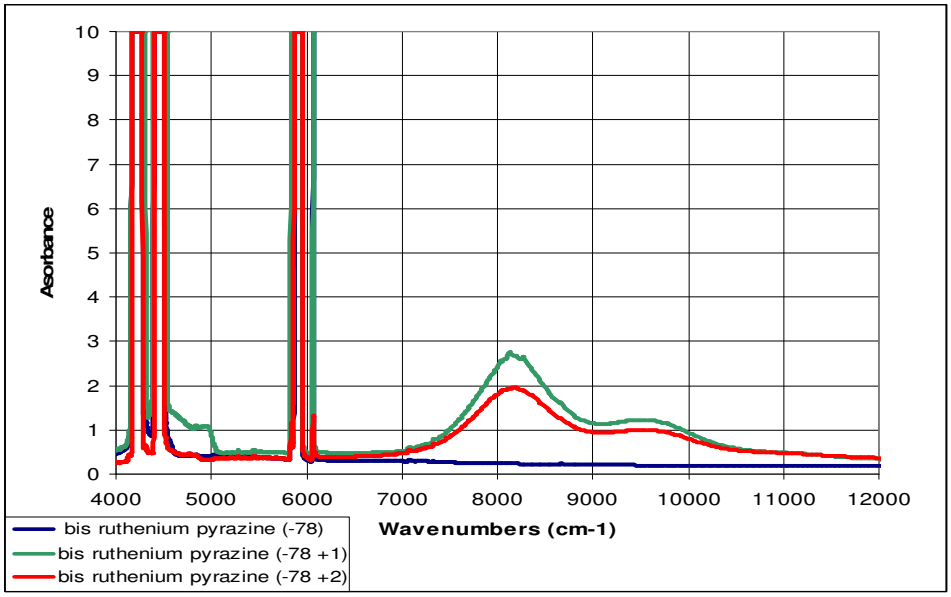

Figure 27- Diagram illustrating spectral subtraction for complex 15^{+} and 15^{2+}

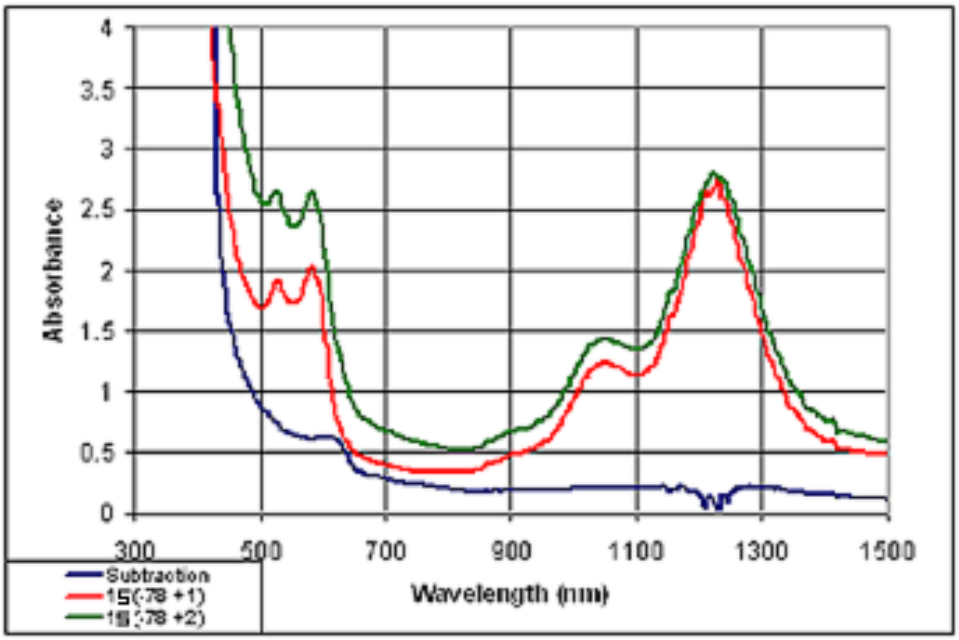

Summary:

As stated previously, there exist nanowires and nanotransistors. These two components are important in circuitry and electronics. In order to connect the two components, a connectable molecular component must be synthesized that will complete the circuit. The significance of the project is that if successful it can compete with the current silicon-based technology that many of the electronics are built from. The size of electronics could be greatly reduced, the costs will be decreased, and perhaps efficiency will be improved. The applications range from disposable DVDs and CDs to flexible LCD screens.

The building block of chemistry and matter is called the atom. The atom consists of neutrons, protons and electrons. Each element is comprised of its characteristics atoms. The group aims to synthesize a compound, a substance made up of more than one element, that will be able to connect the nanowires and nanotransistors. The template for the compound is to have two ruthenium metal atoms connected by a conjugated organic bridge. Metals are good conductors of heat and electricity. Organic compounds are compounds that are carbon based and often contain other non-metals such as hydrogen and oxygen. Conjugated organic compounds in this project have double bonds that alternate and studies have shown that it helps conduction of electricity.

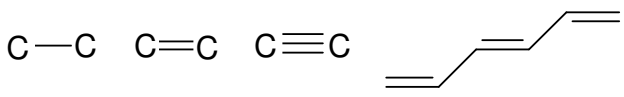

Figure 26- Diagram illustrating the single, double and triple bond and conjugation

The reactions explored in the project were substitution reactions, olefin metathesis for metal incorporation, hydride insertion reactions, and radical reactions. The complexes that are desired are diruthenium complexes but the monoruthenium complexes must be synthesized first. Many of the ruthenium starting materials are commercially available or previously synthesized in the laboratory. In order to synthesize the desired monoruthenium complex, substitution reactions are often used. Compounds that can coordinate or bond to the ruthenium atom are called ligands. These ligands often have free/non-bonded electrons that are important to bond the ligand with ruthenium. Since the ruthenium atom can only accommodate a limited number of ligands, a ligand called the leaving group is replaced by the incoming ligand. The incoming ligand is the ligand that researchers are interested in and it is added to the ruthenium complex.

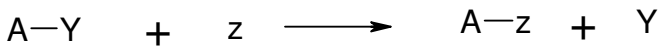

Figure 27- Illustrating the substitution reaction

The choice of ligands is important for the project. Ligands have their own individual properties and so does the ruthenium atom. The properties of the complex, the ruthenium atom plus all the bonded ligands, are determined by the interaction between ruthenium and the ligands. Properties such as stability, reactivity, solubility, absorption, etc. are all affected by the ligands used. Through research of the literature, ligands are carefully selected for the purposes of the project.

Olefin metathesis for metal incorporation is similar to two substitution reactions. An olefin is a compound that contains multiple bonds, while metathesis means exchange. There are two complexes A-B and C-D. The end result is that the complexes A-D and C-B are obtained. The reaction is adapted slightly in this project. There are complexes A-B, C-D and E-E. If both complexes A-B and C-D favor E-E, the end result is the complex A-E-E-C. In this project, A-B and CD are ruthenium complexes while E-E is the conjugated organic backbone. It is a reaction that can synthesize the di-ruthenium complex from the mono-ruthenium complexes.

The hydride insertion is a reaction between a hydride, a ruthenium atom that is bonded to a hydrogen atom and an alkyne, a compound that contains two carbon atoms that are triple bonded. Similar to the olefin metathesis reaction, it provides a route to go from a mono-ruthenium complex to a di-ruthenium complex. In addition, the ligand can be altered to suit the purposes of the project by changing the middle portion of the ligand labeled X in the figure.

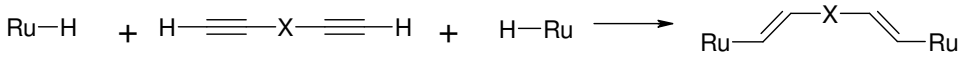

Figure 28- Diagram illustrating the metal hydride insertion reaction

The last reaction to be discussed is the radical reaction. The radical reaction involves a class of elements called halogens. The halogens are comprised of the elements chlorine, fluorine, bromine and iodine. The most popular are chlorine and bromine because they are easier to use,

handle and control. The radical reaction used in this project is called a halogenation reaction. It is a reaction that allows the substitution of a group on a compound by a chlorine atom. Chlorine is a good leaving group, thus it makes future substitution reactions more favorable.

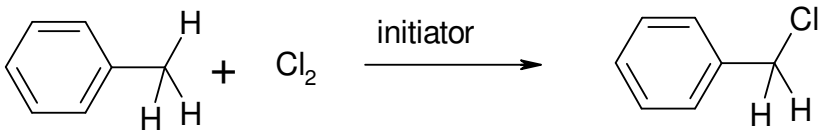

Figure 29- Diagram illustrating the radical halogenation reaction

In order to monitor and identify the progress of a reaction, nuclear magnetic resonance spectroscopy (NMR) and infrared spectroscopy were used. In the case of NMR spectroscopy, information regarding the environment of the hydrogen atoms in a compound is interpreted to yield the identity of the compound. In IR spectroscopy, since bonds are elastic, the vibrations and motions in a bond tell us information about the elements in the compound since vibrations are specific to the elements in the bond. In addition, ultraviolet visible spectroscopy and cyclic voltammetry are characterization methods that determine whether the electronic properties and redox properties are suitable for use as connectable molecular components.

After conducting the reactions and analyzing the results obtained, there were obstacles encountered. The main obstacles were that the complexes synthesized often decomposed and were not stable. Two other problems were that the complexes were difficult to synthesize and solubility made it difficult to characterize the complexes. Despite these

problems, there was some success in that some complexes with potential were obtained. In addition, the results of the project and information obtained will be useful in the future. There are numerous other methods, reactions and possibilities to the project and only a minute fraction has been examined here. It remains probable that a solution will appear for this problem given the number of options available and the number of people working on the problem.